Novel Mechanisms of Tubulointerstitial Fibrosis

MSc (by Research)

2017

Faculty of Science of Engineering

School of Healthcare Science

Callum McDowall

A thesis submitted in fulfilment of the requirements of the Manchester Metropolitan University for the degree of Master of Science (by Research)

Contents

Table list:

Figure list:

Abstract

Kidney disease affects 8.8% of people over the age of 18 in the UK and represent a significant public and a financial burden for the National Healthcare Service (NHS). Untreated Chronic kidney disease (CKD) can develop into end-stage renal failure, leading to costly dialysis or kidney transplantation.

One of the major causes of CKD is diabetic nephropathy, which is characterised by the progressive degradation of nephrons within the kidney as a result of type 1 and type 2 diabetes. One of the major pathways that drives the progression of CKD is Tubulointerstitial Fibrosis (TIF), which is linked to excessive Extracellular Matrix (ECM) accumulation in the tubules of the kidney nephrons and is considered an irreversible process. Currently there is no treatment for TIF and research needs into new targets and treatment strategies that can lead to prevention or even reversal of TIF. MicroRNAs (miRNAs) regulate protein expression by forming a RNA-induced silencing complex (RISC) and targeting specific mRNAs for degradation, the up or downregulation of miRNAs can heavily influence the progression of diseases making them a crucial area of research, as the inducing or blocking the activity of certain miRNAs could slow or halt disease progression.

Therefore, the aim of this project was to identify novel fibrosis-related miRNA targets for treatment of CKD by exposing Renal Proximal Tubular Epithelial Cells (RPTEC) to sera of patients with different stages of diabetic nephropathy.

To investigate the effect of serum factors in patients with diabetic nephropathy on initiating TIF, human renal proximal tubular (HK-2) cells were exposed for 24h or 48h to sera from 16 patients at different stages of CKD or sera from age and gender matched healthy volunteers. Then the effects of 1% human serum on cell viability, Plasminogen activator inhibitor-1 (PAI-1) reporter gene assay, PAI-1 and collagen 1 protein expression, and the regulation of 84 fibrosis-related miRNAs were studied.

The results demonstrated that progressive stages of CKD reduced cell viability, increased the protein expression of PAI-1 and collagen-1 (in particular by stage 4 CKD sera), and dysregulated the expression of a number of fibrosis related miRNAs at 24h or 48h of exposure to serum. A number of miRNAs were up- or down-regulated by sera from patients with different stages of CKD, particularly those related to signal transduction and transcriptional regulation, as well as pro-fibrotic miRNAs. Of particular interest for further investigations are the following miRNAs that were upregulated both at 24h and 48h: miR-449b-5p (the only miRNA upregulated by all patient sera), miR-122-5p (the only miRNA upregulated by sera of CKD 3a stage patients) and miR-217 (the miRNA down-regulated much more severely than any others).

In conclusion, this project demonstrated that the increasing stage of CKD in patients with diabetic nephropathy has a detrimental effect on proximal tubular cells *in vitro* and dysregulates the expression of fibrosis-related miRNAs. Further research is required to identify the genes regulated by key miRNAs and to determine their suitability as therapeutic targets in treating TIF and CKD.

1 Introduction

1.1 Kidney disease

Acute and chronic kidney diseases are costly for the NHS. They affects 8.8% of people aged 18 and over in the UK, and about 1.3% of the NHS budget is spent on treating kidney disease.

Chronic kidney disease (CKD) is caused by different factors, the main being diabetes mellitus and hypertension (Nasri and Rafieian-Kopaei, 2015). These can lead to kidney damage by inducing the progressive loss of functioning nephrons, which is one of the main characteristics of CKD (Schnaper, 2014). If left untreated, CKD can develop into end-stage renal disease (ESRD), which requires costly and life altering treatments such as dialysis or a kidney transplant. The hallmark of CKD is the progressive destruction of the renal tubules in the process of tubulointerstitial fibrosis.

1.2 The Nephron and the Renal proximal tubular epithelial cell

Within the kidney the process of filtering waste products from the blood occurs in independent units called nephrons (Kurts et al., 2013). There are about a million nephrons in each kidney, and each one consists of a glomerulus and tubules. The glomerulus contains a mesh of fine capillaries wrapped up by podocytes, glomerular basement membrane, intercalating mesangial cells, and the Bowman's capsule (Figure 1). The main function of the glomerulus is the filtration of primary urine. The content of the primary urine in healthy people is close to serum plasma with the exception of proteins with molecular weight higher than 60-100 kDa (Tojo and Kinugasa, 2012). The primary urine is concentrated to final urine as it passes through a single tubule that leaves each glomerulus. The tubule consists of several segments (proximal tubule, loop of Henle, and distal tubule), each with defined functions.

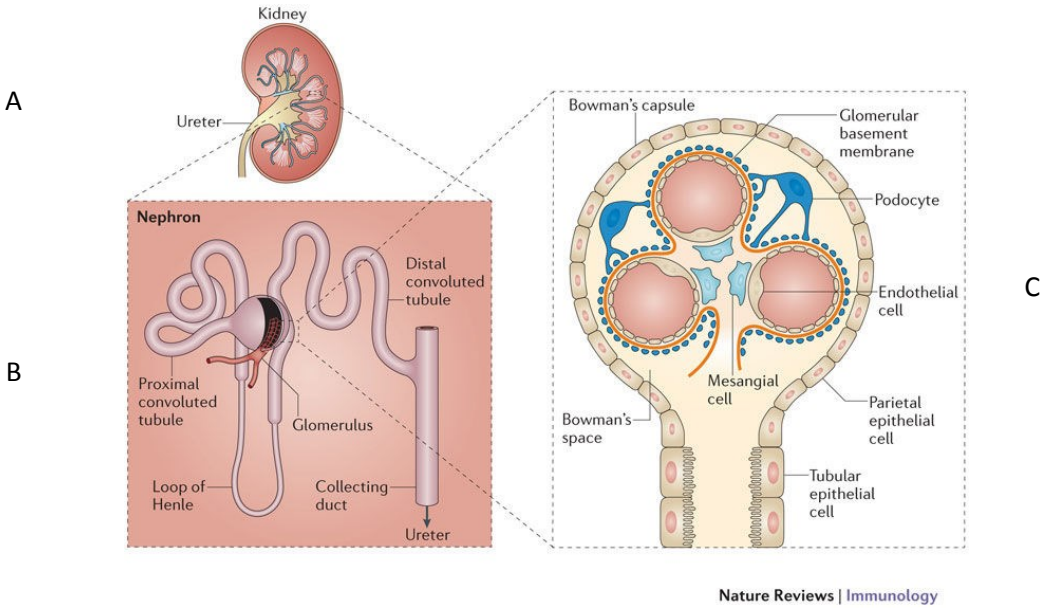

Fig.1: **Basic kidney morphology** (Kurts et al., 2013)
A: Gross morphology of the kidney showing the renal cortex, renal medulla, renal pelvis and ureter. B: Structure of the nephron: glomerulus with afferent and efferent arterioles, proximal convoluted tubules, loop of Henle, distal convoluted tubules and collecting duct. C: A cross section of the glomerulus demonstrates the structure of the Bowman's capsule and the location of the capillaries, podocytes, glomerular basement membrane, and mesangial cells in relation to the proximal tubular epithelial cells.

Located within the nephron between the Bowman's capsule and the loop of Henle, the renal proximal tubular epithelial cells (RPTEC) are essential in normal kidney function. They play a major role in reabsorption of glucose, proteins and amino acids, and substances such as calcium and magnesium and excretion of metabolic waste and xenobiotics. The RPTEC also maintain the pH homeostasis by excreting bicarbonate and synthesising of ammonia (Van der Hauwaert et al., 2013). The important homeostatic function of the RPTEC is underlined by the fact that damage to the proximal tubular cells that leads to tubulointerstitial fibrosis is the key factor driving the progression of CKD to ESRD.

Injury to the proximal tubular cells can induce them to secrete pro-inflammatory and a pro-fibrotic effectors. Proteins such as albumin and immunoglobulin G (IgG) which can be present in the urinary filtrate are able to stimulate the proximal tubular cells to express inflammatory molecules and chemokines (Tang and Neng Lai, 2012). This can happen through the activation of several pathways, including nuclear factor kappa B (NF-κB) and p38 mitogen-activated protein kinases. The activation of these pathways can result from hyperglycaemia (Duran-Salgado and Rubio-Guerra, 2014), which is a hallmark symptom of diabetes. Prolonged hyperglycaemia causes generation of Advanced Glycation End products (AGE) and increases oxidative stress within the kidney, leading to production of reactive oxygen species and the activation of the renin-angiotensin system. This activation increases the levels of angiotensin-II, endothelin-1 and urotensin-II (Lim, 2014), the imbalance of levels leads to vasoconstriction and the production of pro-inflammatory and pro-fibrotic molecules through the MAPK signalling cascades.

1.3 Diabetes and kidney disease

Both type 1 (insulin-dependent) and type 2 (insulin-resistant) diabetes can cause renal damage, which can lead to diabetic nephropathy. Diabetic nephropathy (DN) is characterised by the abnormal levels of urinary albumin and structural and functional changes within the glomeruli (Lim, 2014). The damage to the nephrons causes increased proteinuria (excessive amount of protein in the urinary filtrate) and decreasing glomerular filtration rate. The increased amount of filtered protein directly (by inducing harmful signalling cascades) or indirectly (through increased protein reabsorption and catabolism) can damage the RPTEC, thus leading to decreased kidney function.

DN causes mesangial expansion and nodular glomerulosclerosis which cause the basement membrane to thicken (Lim, 2014). A significant reason for this change is the increased recruitment and activation of immune cells within the kidney. Tubular epithelial cells produce chemokines such as Monocyte Chemoattractant Protein-1 (MCP-1), Colony Stimulating Factor-1 (CSF-1) and Intracellular Adhesion Molecule-1 (ICAM-1) in response to specific cell signalling cascades. These cascades include Mitogen-Activated Protein Kinases (MAPK) and Protein kinase C-β and activate nuclear factor kappa B (NF-κB). The chemokines released attract and promote infiltration of monocytes from the circulating blood as well as differentiation of monocytes into macrophages. Once activated the macrophages assist to progressive DN by the release of inflammatory cytokines and profibrotic cytokines leading to factors such as oxidative stress, fibroblast activation and further inflammation, all of which will cause renal injury and contribute to the development of CKD.

Chronic kidney disease can be classified into stages according to estimated glomerular filtration rate (eGFR) which is the rate of ultrafiltration of plasma from blood into Bowman's space as it traverses the glomerular capillaries (Levey et al., 2015). The stages of CKD are numbered from 1 to 5 (Thomas et al., 2008):

- Stage 1: normal eGFR ≥ 90ml/min per 1.73m^2
- Stage 2: eGFR between 60 to 89ml/min per 1.73m^2

- Stage 3a: eGFR between 45 to 59ml/min per 1.73m^2
- Stage 3b: eGFR between 30 to 44ml/min per 1.73m^2
- Stage 4: eGFR between 15 to 29ml/min per 1.73m^2
- Stage 5: eGFR of < 15ml/min per 1.73m^2

CKD causes many complications during its progression to end stage renal failure, which increase in effect as the stages advance. A normochromic, normocytic anaemia usually accompanies CKD (Thomas et al., 2008), this can arise from the decreased secretion of the hormone erythropoietin from the kidney which is essential to the growth of red blood cells. The tubular atrophy caused by the progressing CKD leaves less capacity for erythropoietin synthesis, which then leads to anaemia.

Another issue CKD can cause is hyperphosphatemia, this results from renal phosphate excretion being decreased due to reduced production of vitamin D (Hruska et al., 2008). This is generally observed in stage 3 patients and will lead to bone and mineralisation issues such as renal osteodystrophy.

Cardiovascular disease risk is also increased with increasing stage of CKD due to low eGRF and increased albuminuria (Gansevoort et al., 2013). The lower eGFR leads to left ventricle hypertrophy, which is thought to be caused also by increased inflammation and high levels of C-reactive protein and fibrinogen. The increased risk is also partially assisted by CKD complications such as hypertension and diabetes (Dervisoglu et al., 2012).

1.4 Tubulointerstitial fibrosis

Tubulointerstitial fibrosis (TIF) is the hallmark of CKD progression, regardless of the initial cause (Efstratiadis et al., 2009). It is characterised by the abnormal accumulation of extracellular matrix (ECM) proteins (e.g. collagens) in the renal interstitium, which is the space between the tubules. The excessive ECM deposition leads to a cycle of inflammation where the macrophages cause the epithelial cells to secrete inflammatory chemokines such as Interleukin-1 (IL-1), IL-6 and TGF-β, which will further increase inflammation leading to the decreased function of the kidneys (Michael Zeisberg and Neilson, 2010). Other elements of ECM contribute to TIF development, such as the increased expression of tissue transglutaminase which is involved in stabilising and increasing protease degradation resistance in the ECM (Farris and Colvin, 2012).

TIF can undergo 4 phases (Loeffler and Wolf, 2014): first, the injury phase when cells are activated and populate the interstitium where they release pro-inflammatory and injurious molecules, followed by the second phase when fibrosis promoting factors like TGF-β1 are produced. The third phase is when ECM production is increased and matrix degradation is decreased which leads to the final phase when nephrons are continuously destroyed and renal function declines.

In diabetes the major triggers of TIF are hyperglycaemia and inflammation coming from the kidney injury. Hyperglycaemia promotes the production of TGF-β1 through activating the protein kinase-C pathway, increasing AGE production and oxidative stress. They activate the renin-angiotensin system and lead to the production of further pro-fibrotic factors (Wolf, 2006). The infiltration of macrophages in the tubulonterstitium causes the recruitment of more macrophages through the activity of chemokines such as ICAM-1 and MCP-1. The macrophages also recruit fibroblasts which altogether leads to the excessive build up of ECM. These triggers are apparent in DN patients which affected all the patients involved in this research.

1.5 Epithelial to Mesenchymal Transition (EMT)

Fibroblasts are connective tissue cells which are derived from the mesenchyme (Brohem et al., 2013) and contributes heavily to the increased ECM. They represent a large portion of the cells in the renal interstitium, alongside dendritic cells, macrophages and lymphocytes (M. Zeisberg and Kalluri, 2015). Fibroblasts can attach to injured tubular basement membrane and change phenotype into myofibroblasts which are responsible for the production and accumulation of Collagen-I and Collagen-III (Fujigaki et al., 2005). As well as fibroblasts, bone marrow fibrocytes that are circulating in the blood are recruited to the interstitium (Yan et al., 2016). The recruitment is due to chemokines such as Chemokine Ligand-2 (CCL2) which is secreted by injured cells and macrophages, the fibrocytes express a certain chemokine receptor Chemokine Recptor-2 (CCR2) which is found to be a receptor to CCL2 (Sakai et al., 2010). Fibrocytes produce ECM due to stromal cell markers such as Collagen-1 and CD34 that can be detected on the cells and fibrocytes are found in injured kidneys (Meran and Steadman, 2011). TGF-β1 and MCP-1 is also thought to be produced by fibrocytes but the action of fibrocytes is still not fully explored but may be an important contributor to fibrosis.

A major mechanism contributing to TIF is Epithelial-Mesenchymal Transition (EMT) where epithelial cells are transitioned into mesenchymal myofibroblast cells (Zhao et al., 2013). The mechanism involves epithelial cells losing markers such as E-Cadherin and cytokeratin and then expressing mesenchymal markers such as α-smooth muscle actin (α-SMA). The mechanisms of this process have not been fully understood but it is thought that certain transcriptional factors and signalling pathways play a role, particularly those that repress E-Cadherin. The activity of Snail1 is one such protein that is theorised to cause E-Cadherin suppression as it binds to E-Cadherin promoter regions and represses expression of it (Michael Zeisberg and Neilson, 2009). The expression of Snail1 depends on β-Catenin, which plays a role within EMT, it controls the expression of Snail1 through the formation of a complex with T cell factor.

The increased accumulation of ECM is also aided by the induced expression of the matrix metalloprotease 9 (MMP-9) gene; this disrupts tubular basement membranes by the cleaving of Collagen-IV and Laminin. It is also thought that MMP-9 is involved in the activation of TGF-β1 which as discussed is pivotal in the mechanisms of TIF such as inducing EMT (Zhao et al., 2013). This induced gene expression is thought to be caused by tissue plasminogen activator (tPA) (Farris and Colvin, 2012).

Tubular epithelial cells are thought to contribute to increased extracellular matrix with the process EMT (Farris and Colvin, 2012) due to acute damage to the cells from the increased oxidative stress (Meran and Steadman, 2011). During this process cells lose epithelial markers and acquire mesenchymal markers which increases the motility of the cells and allows them to move into the interstitium where they add to the ECM.

1.6 PAI-1 and Tubulointerstitial Fibrosis

The *Plasminogen activator inhibitor-1 (PAI-1)* gene is located on the chromosome 7q21.3-q22 in humans (Ghosh and Vaughan, 2012) and produces a protein of 45 kDa. PAI-1 can be synthesised by different cell types such as macrophages, cardiomyocytes and also renal proximal tubular epithelial cells. There are other forms of PAI (e.g. PAI-2 and PAI-3), which have more localised expression. For example, PAI-2 is found in high levels in placental matter (Ghosh and Vaughan, 2012) and is thought to be important in placental tissue homeostasis and foetal growth regulation. PAI-3 is synthesised in the liver and may be important in regulating male reproductive tissue.

PAI-1 protein expression is upregulated by high glucose and TGF-β1 (Lee and Ha, 2005). TGF-β1 effect on PAI-1 expression is mediated by reactive oxygen species (ROS) which, as discussed before, are a major factor in the progression of diabetic nephropathy. TGF-β1 induces PAI-1 expression via the action of p53 and Smads which form a complex to activate the transcription of the *PAI-1* gene (Kawarada et al., 2016).

PAI-1 protein is expressed as a stable inactive form, and when activated, it binds to the active sites of the urokinase plasminogen activator (uPA) and tissue plasminogen activator (tPA) (Eddy and Fogo, 2006). uPA and tPA are the primary activators of plasminogen into plasmin and facilitate fibrinolysis. Inhibition of uPA and tPA inhibits the degradation of ECM components, leading to accumulation of ECM. As shown in Figure 2, on tissue level the main role of PAI-1 is to assists wound healing by preventing the degradation of ECM through the inhibition of tPA and uPA (Ghosh and Vaughan, 2012).

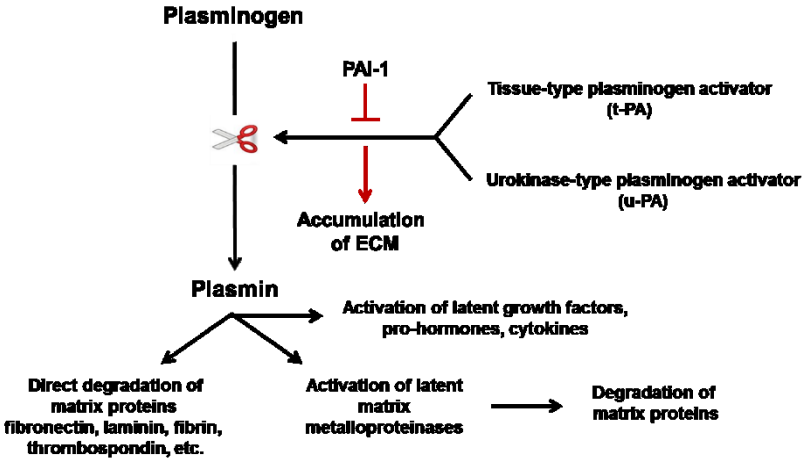

Fig.2: Role of PAI-1 in plasminogen activation and regulation of ECM turnover
PAI-1 regulates the ECM turnover by inhibiting the activity of t-PA and u-PA. t-PA and u-PA activate plasminogen into plasmin which causes the degradation of ECM by several mechanisms, including the activation of matrix metalloproteinases. The inhibition of t-PA and u-PA by PAI-1 causes the excessive build-up of ECM by inhibiting plasmin activation.

The build-up of ECM proteins is a key feature of TIF and is exacerbated by higher level of PAI-1 thus making PAI-1 a suitable marker for tissue fibrosis. It has been found that PAI-1 is overexpressed in the glomerular mesangial cells of diabetic nephropathy patients (Lee and Ha, 2005). The high levels of glucose and the increased TGF-β lead to overexpressed PAI-1 within the kidney making it an important marker in research involving diabetic nephropathy.

1.7 Collagen-I and Tubulointerstital Fibrosis

Collagen-I is a major component of the ECM accumulated during fibrosis in general so it can be used as a marker of fibrosis. The cause of the increased collagen during fibrosis is thought to be from myofibroblasts arising from processes such as EMT (Chen and Raghunath, 2009) and endothelial-to-mesenchymal transition (EndMT). EndMt is stimulated by TGF-β2 with TGF-β3 being involved in the invasion and migration of the cells into the underlying tissue. EMT and EndMT are also thought to be induced by the Collagen-1 by the activation of the signalling receptors α2β1 integrin, discoidin domain

receptor 1 and 2 (Medici and Kalluri, 2012). Within glomerulosclerosis, there is Collagen-I and III expression that's thought to be related in the late stages of glomerulosclerosis and the development of the Kimmelstiel-Wilson nodules which are large deposits of matrix within the nephron (Mason and Wahab, 2003).

1.8 The effect of Cytokines on ECM production

Cytokines are proteins produced by a broad spectrum of cells and can influence cell actions and cell interactions (Zhang and An, 2007) in an autocrine, paracrine or endocrine way. In CKD cytokines are produced by a variety of renal and endothelial cells and paly an essential role in renal fibrosis.

The key cytokine that drives renal fibrosis is Transforming Growth Factor beta (TGF-β). TGF-β is essential for the process of tissue repair. However, overexpression of TGF-β has been linked to abnormal ECM accumulation by renal and endothelial cells (Loeffler and Wolf, 2014). In endothelial cells, TGF-β can regulate cell proliferation and cell apoptosis, and contributes to the production of myofibroblasts by the process of EndMT (Loeffler and Wolf, 2014), which leads to increased ECM in the interstitium. TGF-β has also been shown to cause injury to tubular cells through transcriptional regulation of apoptotic factors, increasing the levels of reactive oxygen species which precedes apoptosis (Gentle et al., 2013). RPTECs have been shown to secrete TGF-β when stimulated by albumin, which in kidney disease high levels of albumin is a hallmark (Tang and Neng Lai, 2012). As discussed before the production of TGF-β is heavily linked with diabetic nephropathy with the redox imbalance causing a cycle of TGF-β1 activation and production and also affecting PAI-1 production through via the action of p53 and Smads which form a complex to promote the activity of *PAI-1* gene (Kawarada et al., 2016).

1.9 MicroRNAs and Tubulointerstital Fibrosis

MicroRNAs (miRNAs) regulate protein expression by forming a RNA-induced silencing complex (RISC) and targeting specific mRNAs for degradation (Wahid et al., 2010). miRNAs are organised in genes, which transcribed to a primary miRNA. The primary miRNA is cut into precursor miRNAs (pre-miRNA) within the nucleus by the class 2 RNase III enzyme Drosha (Wahid et al., 2010). The pre-miRNAs are then transported into the cytoplasm by the nuclear transport receptor exportin-5 and processed into 21-25 nucleotides long mature miRNA by RNase III Dicer. RISC is formed in expectation of a target complementary mRNA for silencing (Ha and Kim, 2014).

The expression of miRNAs is highly regulated and they can affect different processes such as cell proliferation, death, immunity and fibrosis. The general function of miRNAs are in gene regulation by targeting and inhibiting the translation of specific complementary mRNAs leading to decreased translation of the target protein. Furthermore, evidence suggests that miRNAs can also upregulate gene expression (Orang et al., 2014), but this is specific to cell type and the presence of certain factors.

miRNAs are essential for normal kidney homeostasis. It has been shown that podocyte specific inactivation of Dicer can induce kidney failure through proteinuria and glomerulosclerosis (Patel and Noureddine, 2012). While the miRNA involvement in this process is not fully understood, it has been suggested that they play a role in preventing it. Furthermore, particular miRNAs seem to be involved

in TIF, either by being up- or down- regulated by TGF-β or by regulating the TGF-β axis. It has been demonstrated that TGF-β1 induced miR-192 up-regulation increased collagen production in diabetic mice (X. Jiang et al., 2010), while down-regulation of miR-200 promotes the expression of TGF-β2 which leads to EMT (Patel and Noureddine, 2012). Research has been conducted into the expression of miRNAs with proximal tubular cells (Kito et al., 2015). It was found as discussed that miR-200 and miR-192 were found to be significantly increased after acute kidney injury.

1.10 miRNA Potential therapies

As miRNAs are involved in TIF progression there could be potential in suppressing or delivering specific miRNAs to reduce ECM production and slow the progression of CKD or even reverse kidney disease. As mentioned above, specific fibrosis-related miRNAs have been found to be upregulated in kidney injury. Although blocking the activity of these specific miRNAs can halt the progression of CKD, research in this area is still limited. There is evidence that specific antibodies can block the action of miRNAs, and inhibition or delivery of miRNAs can suppress adverse effects in cultured cell models (Shi and Shi, 2011). Despite obstacles in the delivery of miRNA and antibodies to the target cells due to their instability in the circulation (Baumann and Winkler, 2014), it is important to continue the research into novel mechanisms leading to TIF and CKD.

1.11 Aims and objectives

The aim of this study is to identify novel fibrosis-related miRNA targets for treatment of CKD by exposing RPTEC to sera of patients with different stages of diabetic nephropathy.

To achieve that, the following objectives were pursued in this research project:

1. To develop and validate a cell based system for high-throughput screening of fibrosis using immortalised human RPTECs (HK-2 cells) transfected with a soluble luciferase reporter gene under the transcriptional control of *PAI-1* promoter.
2. To test the effects of sera from volunteers and patients with CKD on the transcriptional activation of *PAI-1* promoter and the protein expression of collagen-1 and PAI-1 in HK-2 cells.
3. To examine the dysregulation of fibrosis-related miRNA expression in response to patient sera in HK-2 cells.

2 Methods

2.1 Human serum samples from patients and volunteers

2.1.1 Patient serum samples

Anonymised sera from 16 patients with diabetic nephropathy and kidney disease stages from 3a to 5 were provided by the Nephrology Department of the Salford Royal Trust (Table 1). NHS ethical approval and informed consent were obtained for this study by the Salford Royal Trust. The samples were collected in 3.5ml silica coated BD Vacutainer bottles with Hemogard stops. The samples were then centrifuged for 10 minutes at 2000g and then stored at -80°C.

Table 1: Patient age and CKD stage

Patient number	Age	CKD stage
P-01	40	3a
P-02	50	3a
P-03	56	3a
P-04	59	3a
P-05	46	3b
P-06	58	3b
P-07	42	3b
P-08	53	3b
P-09	38	4
P-10	55	4
P-11	40	4
P-12	45	4
P-13	57	5
P-14	59	5
P-15	61	5
P-16	58	5
Mean age	51 (± 8)	

2.1.2 Volunteer recruitment and specimen collection

The study was approved by the MMU ethics committee. Age and gender matched healthy volunteers were recruited at the MMU campus and a screening questionnaire was used to select suitable volunteers. Informed consent was provided by the volunteers before blood and urine collection. The samples were anonymised and all the volunteer and patient details were kept confidential.

Seven gender and age matched volunteers were selected for the study and serum and urine samples were collected after overnight fasting. The height and weight of the participants was measured, and the fasting blood glucose levels were measured using the Accu-chek Aviva Blood glucose meter (Williams Medical: W707) (Table 2). Twenty ml of blood were taken from each volunteer via venepuncture by a trained phlebotomist in 2 BD Vacutainer® plastic serum tubes (BD: 367895). The tubes were inverted 5-6 times then left at room temperature for 60 minutes. The blood was centrifuged at 1,300g for 10 minutes at 25°C and serum aliquots of were stored at -80°C.

Urine samples were provided by the volunteers in sterile containers. The urine was centrifuged for 10 minutes at 1,000g and pH, protein concentration and glucose were measured using the Valutest 13

Parameter Urinalysis Reagent Strips (Williams Medical: D2207). The values for each volunteer were within the normal range of the tests. Aliquots of urine were stored at -80°C.

Table 2: Volunteer age, fasting blood glucose and Body Mass Index

Volunteer Number	Age	Blood glucose level (mM)	Body Mass Index (BMI)
V-01	42	5.1	29.8
V-02	57	5.1	20.9
V-03	35	4.9	29.4
V-04	45	4.6	20.8
V-05	60	5.3	25.0
V-06	60	5.6	25.1
V-07	53	5.9	23.5
Mean age	50 (± 9.75)		

2.2 Cell culture

2.2.1 Cells and media

Commercially available human renal proximal tubular cell line HK-2 cells (ATCC® CRL-2190™) were used in all experiments. The cells were maintained in growth media consisting of 6-10% Foetal Calf Serum (FCS), 50:50 DMEM (Dulbecco's Modified Eagle Media):Ham's F12 Medium, 500U/ml Penicillin Streptomycin and 2mM Glutamine. The media were prepared within a sterile environment and stored at 4°C. The cells were supplemented with fresh medium every 2-3 days until the cell confluence reached 80-90%.

Serum free media (SFM; DMEM:Ham's F-12 supplemented with penicillin/streptomycin) was used to growth arrest the cells when they had reached appropriate confluency.

2.2.2 Splitting and seeding cells

The HK-2 cells were grown in a T75 flask at 37°C with 5% CO_2 and 10 ml of growth medium. Upon reaching around 80-90% confluency, the cells were rinsed twice with sterile Phosphate buffered saline (PBS) to remove any cell debris. The cells were detached using 0.25% trypsin-EDTA with Phenol red (Gibco; 25200-056) and the detachment process was monitored using a light microscope.

The detached cells were then re-suspended in growth medium and were counted using a haemocytometer. The number of cells seeded depended on the type of plate used. For 6-well plates 75,000 cells were seeded with 2 ml of growth medium per well; 16,600 cells were seeded with 1ml of growth media per well in 24-well plates; 8,000 cells were seeded with 200µl of growth media per well in 96-well plates.

2.2.3 *In vitro* model of Acidosis

The HK-2 cells were grown to around 80% confluency and then the growth medium was changed to (SFM) for 24 hours to growth arrest the cells. The media were then replaced with SFM of different pHs.

Bis-Tris solution composed of 0.625M bis-Tris (Fluka 14880) and 0.625M bis-Tris hydrochloride (Sigma 136032) was used to adjust the media to pH 7.4, 7.0 or 6.7. For pH 7.4 the composition of the bis-Tris mixture was 83% bis-Tris and 17% bis-Tris hydrochloride; for pH 7.0 - 35% bis-Tris and 65% bis-Tris hydrochloride; for pH 6.7 the mixture contained 17% bis-Tris and 83% bis-Tris hydrochloride. The SFM was mixed with the respective bis-Tris solution in a 50:1 ratio. The pH was then adjusted using a pH meter to achieve target pHs of 7.4, 7.0 or 6.7 and the media were sterile filtered. For any assays with time points over 24 hours the media were refreshed daily.

2.2.4 Exposure of HK-2 cells to human serum

For western blots and miRNA array experiments 75,000 cells were seeded per well in 6 well plates and 3,000 cells were seeded per well in 96-well plates for viability assays. When the cells reached around 80% confluency, the growth medium was removed, the cells were rinsed with PBS, and growth arrested using SFM. After 24 hours, the cells were rinsed with PBS and were exposed to SFM alone or 1% human serum for 24 or 48.

2.2.5 Cell viability

Cell viability was measured using the Cell Counting Kit-8 (Dojindo, Japan; CCK-8) according to the manufacturer's protocol. Briefly, 3,000 cells were seeded per well in 96-well plates and were cultured in grow medium until reaching 80% confluency. The cells were then exposed to either SFM or 1% human serum for 24h or 48h. After 23 or 47 hours, 10 µl of the kit reagent was added to the cell media and absorbance was measured at 450nm and 650nm every hour for 3 hours using the Multiskan GO plate reader (ThermoScientific; 51119200). The reagent added forms an orange dye when reduced by dehydrogenase activities within the cells. The amount of the dye is proportional to the number of living cells.

2.3 PAI-1 Reporter gene construct and assays

2.3.1 Amplification of PAI-1 promoter sequence and cloning into a luciferase reporter vector

The PAI-1 promoter sequence (955bp long: upstream of the start codon -853bp; downstream +82bp) was amplified using Q5 high fidelity PCR kit (New England Biolabs) and specific primers (Table 3A). The PCR products were separated by after agarose gel electrophoresis, the amplified fragment was excised from the gel and purified, and restriction sites were introduced at the ends using the primers shown in Table 3B.

Restriction enzymes Kpnl and XhoI (New England Biolabs: R3156, R0146 respectively) were used to linearise by double digestion the luciferase reporter vector pNL 2.3 and to create the cohesive ends in the PAI-1 fragment. Small restriction fragments were subsequently removed from the reaction using the Purelink PCR micro kit (Invitrogen: K310010) according to the manufacturer's protocol.

Quick-Stick Ligase kit from Bioline (BIO-27027) was used to ligate the purified restriction digested PAI-1 products and the pNL 2.3 vector and the efficiency of the reaction was determined via agarose gel electrophoresis.

A heatshock transformation was used to clone the recombinant plasmids in High efficiency competent *Escherichia coli* DH5α bacteria (New England Biolabs, UK). The ligation products were added to the

DH5α bacterial suspension and placed on ice for 30 minutes followed by 30 seconds at 42°C, then back on ice for 5 minutes. Successful transformants were selected at 37°C on Luria-Bertani agar with 100 µg/ml ampicillin. Selected colonies were amplified and recombinant plasmid DNA was isolated using the QIAPrep Miniprep kit from Qiagen (27104) according to the manufacturer's protocol.

Table 3: PAI-1 Sequences of PAI-1 amplification and restriction sites primer sequences
A) PAI-1 amplification primers; **B)** Restriction site primers: **GGTACC** - Kpnl restriction site; **CTCGAG** - Xhol restriction site; ***TATGGAC*** and ***TAAGCTTT***: mismatch sequences which facilitate restriction digestion.

A)Amplification Primers	**Primer sequence (5' to 3')**
Forward Primer	GCA GCT CGA AGA AGT GAA AC
Reverse Primer	GTG TGG GTC TTC TTG ACA GC
B) Restriction site Primers	**Primer sequence (5' to 3')**
Forward Primer	***TATGGAGGTACC***GCAGCTCGAAGAAGTGAAAC
Reverse Primer	***TAAGCTTCTGAG***CGTCAGGAATTCAGCTGCTG

2.3.2 Transfection of plasmids into HK-2 cells

Confluent HK-2 cells (80%) were transfected in 6 well plates with a mixture of 12µl Lipofectamine, 150 µl of antibiotic-free SFM and 2.5 µg of the PAI-1 reporter construct or native pNL 2.3 vector. The cells were then incubated for 2 hours at 37°C after which 1 ml of antibiotic-free growth medium was added to each well and the cells were incubated overnight at 37°C in 5% CO_2.

The medium was then replaced with growth medium supplemented with 50 µg/ml of Hygromycin and the cells were incubated for 48 hours. Following this the medium was replaced with growth medium supplemented with 500µg/ml of Hygromycin. The medium was refreshed every 3-4 days while the cells were examined for the formation of foci. Selected recombinant and native pNL 2.3 clones of HK-2 cells were expanded and tested for luciferase expression.

2.3.3 Luciferase Reporter Gene Assay

2.3.3.1 Promega End-point Luciferase assay

Luciferase activity was measured in media from cells transformed with PAI-1 luciferase reporter gene construct. The cells were seeded into 6-well plates and grown to 80% confluence after which the cells were exposed to SFM for 24 or 48 hours. At the end of the treatment the plates were gently swirled and the medium from each well was transferred to an Eppendorf tube. The cells were rinsed with PBS and any residual PBS was removed from the wells. The plates were then stored at -20°C until analysis for total cellular protein was carried out.

The harvested media samples were centrifuged at 900 g for 10 min at 4°C. Distilled water (40 µl) and 10 µl of supernatant were mixed and applied to white 96 well plates suitable for luminescence measurements.

Nano-Glo® Luciferase Assay system (Promega, UK; N1120) was used according to the manufacturer's protocol to measure luciferase activity. Briefly a luciferase buffer solution consisting of Luciferase

buffer and Nanoluc substrate (50:1) were added to each well and left to incubate for 2 minutes at room temperature. The luminescence was measured using a Synergy HT microplate reader (BioTek) and the luciferase intensities were normalised to the total protein content of each well, as measured by a BCA assay.

2.3.3.2 Time course of Luciferase secretion using Nano-Glo assay kit

To be able to analyse the PAI-1 expression in a time course experiment 20 µl of media were removed from each well at the respective time point and luciferase activity was measured as described above.

2.3.3.3 Luciferase activity measured using Coelenterazine substrate

In the course of the experiments, the Nano-Glo® Luciferase Assay system kit was replaced by the coelenterazine luciferase substrate (Gold bio, CZ10) due to its cost-effectiveness. Experiments demonstrated that the two approaches produced similar results although lower luciferase intensity was observed using coelenterazine (data not shown).

One mg/ml stock solution of coelenterazine in methanol was diluted 1:10000 in PBS. The content of the luciferase assay buffer is listed in Table 4.

Table 4: Composition of Luciferase Assay Buffer

Master Luciferase Buffer	Luciferase Assay Buffer
50mM Tris Phosphate, pH 7.8	5ml Master Luciferase Buffer
2mM DTT	3ml Glycerol
2mM EDTA	2ml 10% Bovine Serum Albumin (BSA)
2% Triton X-100	
16mM $MgCl_2$ (added last)	

Prior to the assay, 20 µl of luciferase assay buffer and 40 µl of the coelenterazine substrate solution were mixed and added to 20 µl of undiluted sample per well in a white 96 well plate. The luminescence was read and normalised as described above.

2.4 Serum protein fractionation and Western Blotting

2.4.1 Human Serum fractionation

Human serum was fractionated according to molecular size by the use of two different filter devices: a 100kDa Centrisart 1 Centrifugal ultrafiltration unit (Sigma-Aldrich; 13269E) and a 50kDa Vivaspin 2 ultracentrifuge tube (GE Healthcare; 28-9322-57). The filters were used according to their manufacturer's handbooks. Briefly, 100µl of PBS were applied on the filters and the devices were centrifuged at 1,000g for 5 minutes to remove any trace amounts of glycerine, which could interfere with the results.

Using the 100kDa filter, 600 µl of whole serum was centrifuged at 1,000g for 5 minutes, followed by 20 minutes of centrifugation at 2,000g at 15°C. The filtrate and the concentrate obtained were reconstituted to 600 µl with PBS. The 100kDa filtrate was then filtrated through the 50kDa filter using

the same centrifugation conditions, with the concentrate and filtrate being reconstituted to 600 µl with PBS. The samples were then diluted as required either for subsequent silver protein staining of SDS-PAGE gels.

2.4.2 Silver staining of SDS-PAGE gels

The ProteoSilver™ Silver Stain kit (Sigma-Aldrich; PROTSIL1) was used according to the manufacturer's protocol to evaluate the quality of serum fractionation by detecting proteins separated on SDS-PAGE gels. Briefly, 1 µg of total protein from serum filtrate was mixed with loading buffer, loaded into the wells of 12% discontinuous gels and separated as described in section 2.4.3.2. Upon completion of the SDS-PAGE, the gels were placed into 100 ml of fixing solution for 20 minutes:

Fixing solution:

- 50 ml Absolute ethanol
- 10 ml Glacial Acetic acid (≥99.85%)
- 40 ml Ultrapure water

The gels were developed according to the kit's instructions and images were taken using the ChemiDoc™ Imaging system (BioRad; 17001401). The gels were dried using a gel drying frame (Hoefer: SE1210) as per the manufacturer's handbook.

2.4.3 SDS-PAGE and Western Blot

2.4.3.1 Harvesting of cells in Radio Immunoprecipitation Assay (RIPA) buffer

Following the exposure of HK-2 cells to human serum, the cells were rinsed twice in ice-cold PBS. The cells were then harvested on ice using 160 µl of RIPA buffer composed of:

- 20mM Tris-HCL (pH 7.5)
- 150mM NaCl
- 1% NP-40
- 1% EDTA
- 1% 100x Protease inhibitors (ThermoScientific: 1862209)
- 1% Phosphatase inhibitors (Sigma: P5726)

Following the harvesting procedure the samples were sonicated in an ice-water bath at amplitude 20 twice for 5 seconds using a Vibracell™ ultrasonic processor (Sonics and Materials: VCX-130PB). The cell lysates were centrifuged for 10 minutes at 14,000 g at 4°C, the supernatant was aliquoted and stored at -80°C prior analysis.

2.4.3.2 Sodium Dodecyl Sulfate Polyacrylamide Gel Electrophoresis (SDS-PAGE)

Acrylamide gels were either commercially available or cast in the laboratory. The discontinuous in-house gels were composed of a 12% resolving gel and a 4% stacking gel:

12% Resolving gel (20 ml):

- 8ml Protogel 30% (w/v) Acrylamide, 0.8% (w/v) Bis-acrylamide stock solution (37.5:1) (National Diagnostics: EC-890)
- 5ml Resolving gel buffer (1.5M Tris-HCL, 0.4% SDS, pH 8.8; Natural Diagnostics: EC-892)
- 6.8 ml distilled water
- 200µl 10% Ammonium persulphate (APS)
- 20µl Tetramethylethylenediamine (TEMED)

4% Stacking gel (10 ml):

- 1.3ml Protogel
- 2.5ml Stacking gel buffer (0.5M Tris-HCL, 0.4% SDS, pH 6.8; Natural Diagnostics: EC-893)
- 6.1ml distilled water
- 100µl 10% APS
- 10µl TEMED

In some experiments commercial continuous gradient gels were used (BioRad; 4561083) where the gel percentage ranged from 4-15%.

Between 20 µg and 30 µg of total protein were separated per well for Western blotting experiments. The protein samples were mixed with 4x non-denaturating loading buffer, heated to 95°C for 5 minutes, and then cooled on ice.

The 4x non-denaturating loading buffer was comprised of:

- 0.5 Tris HCL, pH 6.8
- 4% SDS (w/v)
- 40% Glycerol (v/v)
- trace of phenol blue

Two µl of pre-stained protein ladder standard per gel was used as molecular weight marker (ThermoScientific; 26619).

Using a Mini Protean Tetra cell (Bio-Rad; 1658004EDU), the gels were submerged in running electrophoresis buffer (25mM Tris/HCl; 0.1% SDS; 0.192M Glycine). The samples and protein standard were loaded on the gels and current of 12mA per gel was applied until the protein has surpassed the stacking gel at which point the current was raised to 20mA.

2.4.3.3 Western blot

Proteins were transferred from gels onto nitrocellulose membranes by semi-dry electro-blotting apparatus (Biorad; 1703940) using two pieces of thick filter paper soaked in transfer buffer (48mM Tris, pH 9.2; 39mM Glycine; 20% Methanol) along with the gel and an equal sized piece of nitrocellulose membrane (Figure 3).

The electroblotting was carried out for 90 minutes at 45mA per gel. Upon completion of the transfer, the nitrocellulose membranes were submerged for at least an hour at room temperature in blocking buffer that consisted of PBS-Tween 20 (PBS-T) buffer (0.05% (v/v) Tween 20; 1x PBS) and 1% BSA.

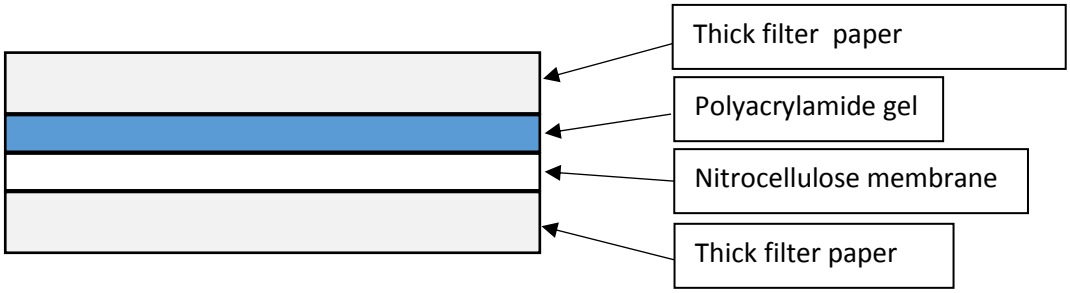

Fig.3. Electrotransfer "sandwich" diagram

2.4.3.4 Detection of target proteins by Western blot

The blocked nitrocellulose membranes were exposed for 90 minutes at room temperature or overnight at 4°C on a seesaw rocker to fresh blocking buffer and primary antibodies to target proteins as shown in Table 5:

Table 5: Primary antibodies used in Western blot

Primary Antibody	Dilution
Mouse IgG against human PAI-1 (BD Biosciences: 612024)	1:1000
Rabbit IgG against human GAPDH (Sigma:G9545-25UL)	1:3000
Rabbit IgG against human Collagen I (abcam:AB34710)	1:3000

The membranes were rinsed 5 times with PBST for 5 minutes to remove any unbound antibody and were then exposed for 45 minutes at room temperature to fresh blocking buffer with a secondary antibody labelled with Horse Radish Peroxidase (HRP) as shown in table 6:

Table 6: Secondary antibodies used in Western blot

Secondary antibody	Dilution
Goat IgG against Mouse (Fab specific)– HRP antibody (Sigma: A9917)	1:5000
Goat IgG against Rabbit (whole molecule)-HRP antibody (Sigma: A0545-1ML)	1:5000
Goat IgG against Rabbit (whole molecule)-HRP antibody (Sigma: A0545-1ML)	1:5000

The membranes were rinsed 5 times with PBST as described before and target proteins were visualised by chemiluminiscence.

2.4.3.5 Enhanced Chemiluminescence (ECL) detection

To visualise target proteins, nitrocellulose membranes were exposed for 1 min to 2ml of ECL solution (ThermoFisher Scientific Pierce™ ECL Western Blotting Substrate kit;32106) as per manufacturer's protocol. Bands were visualised using ChemiDoc™ Imaging system (BioRad; 17001401). Band intensities were measured using Image lab software (BioRad) and analysed with Microsoft Excel.

2.4.4 Protein estimation by BCA assay

Total protein content was measured using a BCA assay kit (Novagen; 71285-30). Cells were harvested in 0.2M NaOH and the lysates were incubated for 2 hours at 37°C. The samples were then centrifuged at 14,000g for 10 minutes at 4°C and were diluted with distilled water. BSA was used as a standard at concentrations of 0, 0.05, 0.1, 0.2, 0.25 and 0.4 mg/ml.

In a 96 well plate 20 µl of standards or samples were added in duplicate were incubated with 200 µl BCA reagent for 30 minutes at 37°C as per manufacturer's recommendations. The absorbance was measured at 570nm on the Multiskan GO plate reader (ThermoScientific; 51119200).

2.5 miRNA expression analysis

2.5.1 miRNA Isolation and purification

mRNeasy mini kit (Qiagen; 217004) was used to isolate and purify miRNA according to the manufacturer's protocol. Briefly, cells exposed to SFM or 1% human serum for 24 or 48 hours in 6-well plates were rinsed with PBS. Cells from 2 wells exposed to the same condition were lysed in 700µl of QIAzol lysis reagent. The lysates were homogenised by pipetting and vortexing, and were stored at -80°C prior to RNA isolation

The lysates were defrosted and 140 µl of chloroform were added to the homogenate. The mixture was shaken until the homogenate and the chloroform were thoroughly mixed, and then it was centrifuged at 12,000g for 15 minutes at 4°C. The upper phase was transferred to a new tube and mixed with 100% ethanol before being pipetted into an RNeasy Mini spin column and centrifuged for 15 seconds at 8,000g. The flow-through was discarded and this step was repeated again.

Then 500 µl of buffer RPE were added to the spin columns and the columns were centrifuged at 8,000g for 15 seconds. The flow through was discarded, another 500 µl of buffer RPE were added and the column was centrifuged again at 8,000g but for 2 minutes. The spin column was transferred to another collection tube and 30 µl of RNase-free water was pipetted directly onto the membrane. The RNA was then eluted by centrifuging at 8,000g for 1 minute and the total RNA content was measured using the NanoDrop™ One^{c} (ThermoScientific; ND-ONEC-W).

2.5.2 Reverse transcription of miRNA

Using the miScript® II RT kit from Qiagen (218160) miRNA-specific cDNA was synthesised from total RNA as per the manufacturer's protocol. Briefly, 20 µl of the reverse-transcription master mix was prepared with:

- 4 µl of 5x miScript HiSpec Buffer
- 2 µl of 10x miScript Nucleics mix

- 2 µl of miScript Reverse Transcriptase Mix
- 1 µg of total RNA

The tubes were mixed gently and briefly centrifuged before being incubated at 37°C for 60 minutes, followed by 5 minutes at 95°C to inactivate the Reverse Transcriptase mix. The samples were were cooled on ice and stored at -20°C.

2.5.3 miRNA qPCR fibrosis arrays

Fibrosis qPCR array (Qiagen; MIHS-117Z, plate diagram shown in appendix 1) was used with miScript® SYBR® Green PCR kit (Qiagen; 218073) to determine the miRNA expression pattern according to the manufacturer's protocol. The following master mix was prepared:

- 1375 µl of 2x Quantitect SYBR Green PCR Master Mix
- 275 µl of 10x miScript Universal Primer
- 1000 µl of RNase-free water
- 100 µl of Template cDNA

All template cDNA obtained from samples exposed to volunteers' serum were mixed together in equal proportions as shown in Table 7 and analysed in a single 96-well qPCR array plate. The cDNA from samples exposed to patient serum were mixed together according to the stage of CKD (i.e. 4 patient samples per 96-well qPCR array plate).

Table 7: Composition of cDNA mixtures for fibrosis PCR arrays

Samples	Number of samples mixed per qPCR array plate	µl of cDNA from individual sample	Total µl of cDNA template	µl of RNase-free water
SFM	1	7 µl	7 µl	100 µl
Volunteers	7	2 µl	14 µl	200 µl
Patients	4	3.5 µl	14 µl	200 µl

The reagents were mixed and 25 µl of the mixture was added to each well in the MIHS-117Z PCR array plate using a multichannel pipette. The plates were tightly sealed using optical adhesive film and were centrifuged at 1,400g for 2 minutes at room temperature before being placed into the StepOnePlus™ Real-Time PCR System (Applied Biosciences; 4376600). The qPCR was carried out following an activation step (15 minutes at 95°C) and 40 cycles at the following settings:

- 15 seconds at 94°C
- 30 seconds at 55°C
- 30 seconds at 70°C

The qPCR programme was followed by the standard for the instrument melting curve programme. The results were analysed using the StepOnePlus™ software v2.3 (Applied Biosciences).

2.5.4 PCR fibrosis array analysis

Amplification and heatmap curves were used to determine the threshold cycle (C_T) for each sample or standard. The baseline and the threshold were determined first and were consistent across all the arrays. The baseline is a section of the cycles which contain only background noise. The baseline start in the analysis was set to cycle 2 and ended at 2 cycles before the earliest noise-free fluorescence increase that could be observed on the linear graph in all array plates. The earlies such fluorescence was detected at cycle 9, therefore, all baseline across all the arrays was set between cycles 2 and 7. The threshold was set to 1000 which positioned it above any background noise in any of the arrays.

Once all the C_T values for all the arrays were calculated, the fold increases for all of the individual miRNA primers were calculated using the miScript miRNA PCR Array Data Analysis program (SabioSciences).

2.6 Statistical analysis

The program SPSS was used to carry out One Way ANOVA with a post hoc Tukey's test which were used to estimate statistical differences between more than 2 independent groups of data. P values of less than 0.05 were considered significant.

3 Results

3.1 PAI-1 reporter gene system

PAI-1 reporter gene system was generated and expressed in HK-2 cells to create a high-throughput approach to testing for the presence of pro-fibrotic factors in a specimen. As the gene reporter system required initial verification and optimisation, first, transfected HK-2 clones were selected and tested for their ability to secrete luciferase.

3.1.1 Selection of pNL2.3 and PAI-1-pNL2.3 HK-2 clones

Following the transfection of HK-2 cells with native pNL2.3 vector or PAI-1-pNL2.3 vector construct, five pNL2.3 clones and twelve PAI-1-pNL2.3 clones were selected, expanded and tested for luciferase expression in serum-free medium (SFM).

As shown in Figure 4A, pNL2.3 clone 1 (pNL1) secreted the least amount of luciferase and was selected as a negative control in all reporter gene experiments. Seven of the twelve HK-2 clones transfected with PAI-1-pNL2.3 construct(PAI1, PAI2, PAI4, PAI5, PAI6, PAI7, PAI9, PAI10 and PAI12) demonstrated a lack of luciferase secretion (Figure 4B). PAI-1-pNL2.3 clones 3, 8 and 11 secreted high levels of luciferase and clone 8 (PAI8) was used in all further reporter gene experiments.

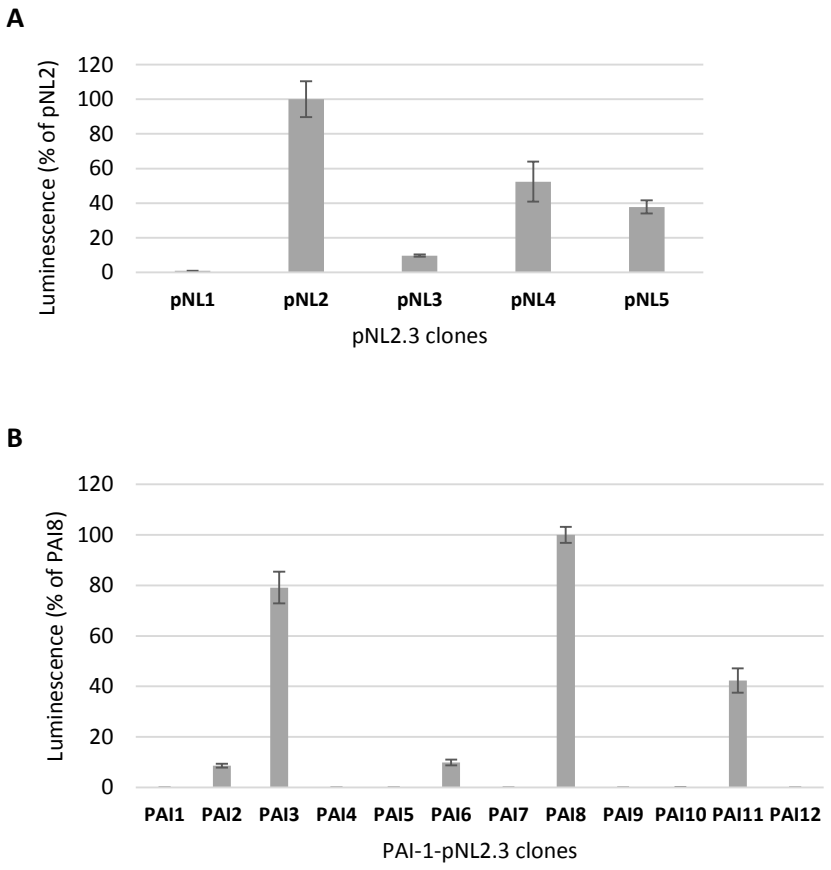

Fig.4. Luciferase activity in media from HK-2 cell clones transfected with pNL2.3 native vector (A) or PAI-1-pNL2.3 vector construct (B) Cells grown in 24-well plates reached 90% confluency and were exposed to SFM for 24 hours. Luciferase activity was measured using an end-point luciferase assay. The data were normalised to total protein content and expressed as percent from the luciferase activity of the most potent clone (pNL2 or PAI8). The raw fluorescence data ranged 0-22,000,000 relative light units (RLU) for the native pNL2.3 clones and 0-1,720,000,000 RLU for the PAI-1-pNL2.3 vector construct.

3.1.2 Time course of Luciferase secretion pNL2.3 clone 1 and PAI-1 clone 8 in response to acidosis

To determine the responsiveness of the reporting gene construct to activation stimuli, cells transfected with pNL2.3 clone 1 or PAI-1-pNL2.3 clone 8 were exposed to SFM with pH 7.4, 7.0 or 6.7 for up to 48 hours. The treatment media were refreshed after 24 hours.

The luciferase activity in cell media increased steadily over the two 24 hours incubation periods regardless of the pH (Figure 5). During the first 24 hours, acidosis (especially pH 6.7) appeared to increase the luciferase expression. However, this effect wasn't observed during the second 24 hour exposure. On the contrary, it appeared that pH 6.7 had a slight inhibitory effect on the expression of luciferase.

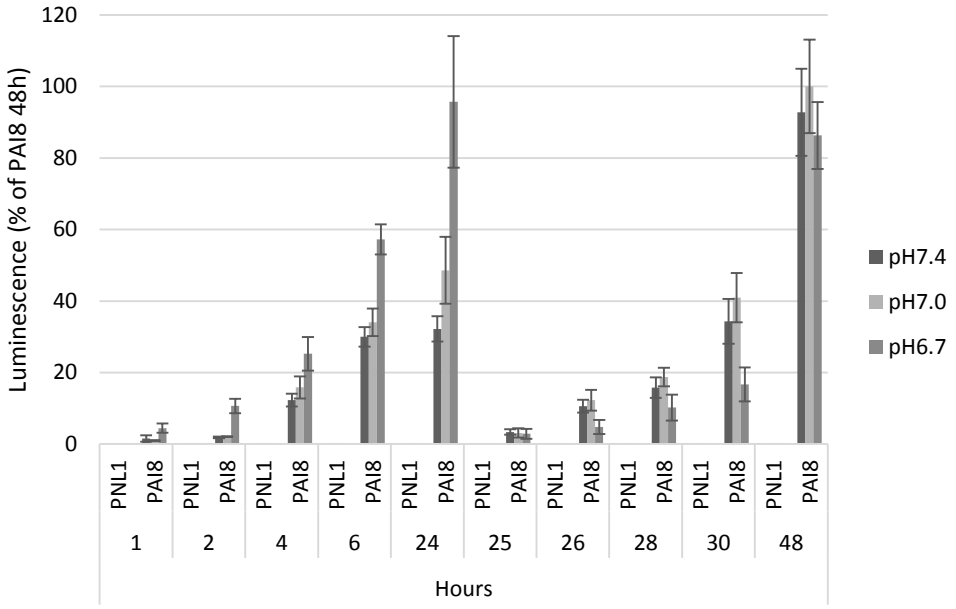

Fig.5. Luciferase activity in media from pNL2.3 clone 1 and PAI-1-pNL2.3 clone 8 cells exposed to pH 7.4, 7.0 or 6.7 for up to 48 hours.

Cells were grown in 6 well plates and luciferase activity was measured in aliquots of treatment media collected at 1, 2, 4, 6, 24, 25, 25, 28, 30, and 48 hours. The luciferase activity was normalised to total protein content and the data are presented as percent from the highest value which was 5,380,000,000 RLU (n=4).

3.1.3 PAI-1 Reporter gene assay in response to human serum

To establish the effect of human serum on PAI-1 promoter activation, PAI-1 clone 8 HK-2 cells were exposed to SFM or 0.1% or 0.5% of volunteer serum for 24h and 48h at which points luciferase activity

Exposure to serum, regardless of the concentration, induced a significant stepwise activation of the PAI-1 promoter as compared to control cells exposed to SFM alone (Figure 6). This effect was observed both at 24h and 48h.

There was no significant difference between the effect of 0.1% and 0.5% serum at 24 hours. However, at 48 hours 0.5% serum significantly increased the secretion of luciferase as compared to 0.1% serum.

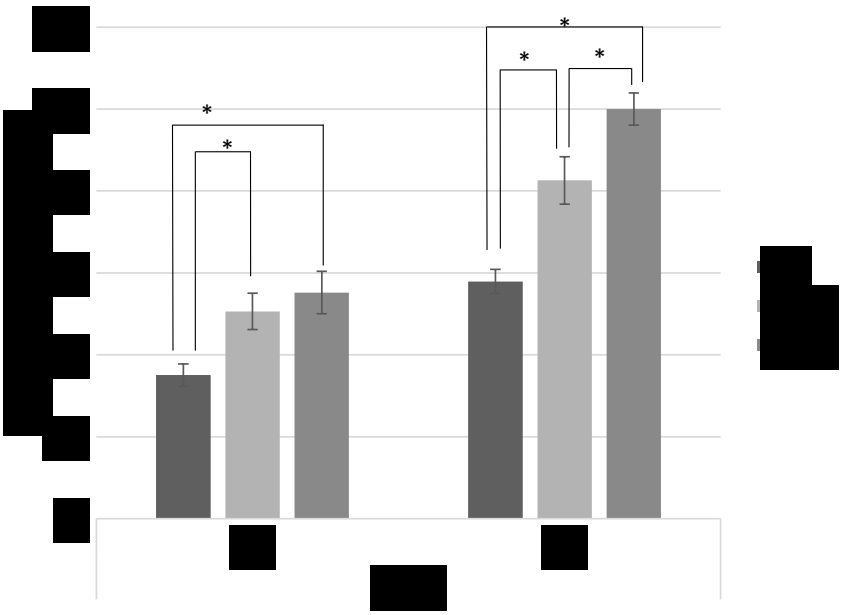

Fig.6. Activation of PAI-1 promoter by human serum

PAI-1 clone 8 cells were exposed to 0.1% or 0.5% human volunteer serum, and media and cells were harvested either at 24h or 48h. The media were refreshed daily. The luciferase activity was measured using the end point luciferase assay method and the data were normalised to total cellular protein in each well. The data are presented as a percentage of the highest value (0.5% serum treatment at 48h) which was 1,084,000,000 RLU. (n=4; *p≤0.05).

3.1.4 PAI-1 Reporter gene assay in response to whole and 100kDa fractionated human serum

To identify the size of serum factors that induced the activation of PAI-1 promter, volunteer serum was fractionated using a 100kDa Centrisart 1 Centrifugal ultrafiltration unit. The resulting <100kDa filtrate and the >100kDa concentrate were diluted to 0.5% or 1% with SFM and exposed to PAI-1 clone 8 cells. Luciferase activity was measured after 24 hours.

As shown in Figure 7, exposure to either 0.5% or 1% of 100kDa concentrate fractions lead to a significant increase in PAI-1 promoter activation, in comparison to SFM, 0.5% filtrate or 1% filtrate fractions. However, there was no significant difference between the effects of 0.5% or 1% 100kDa concentrate fractions.

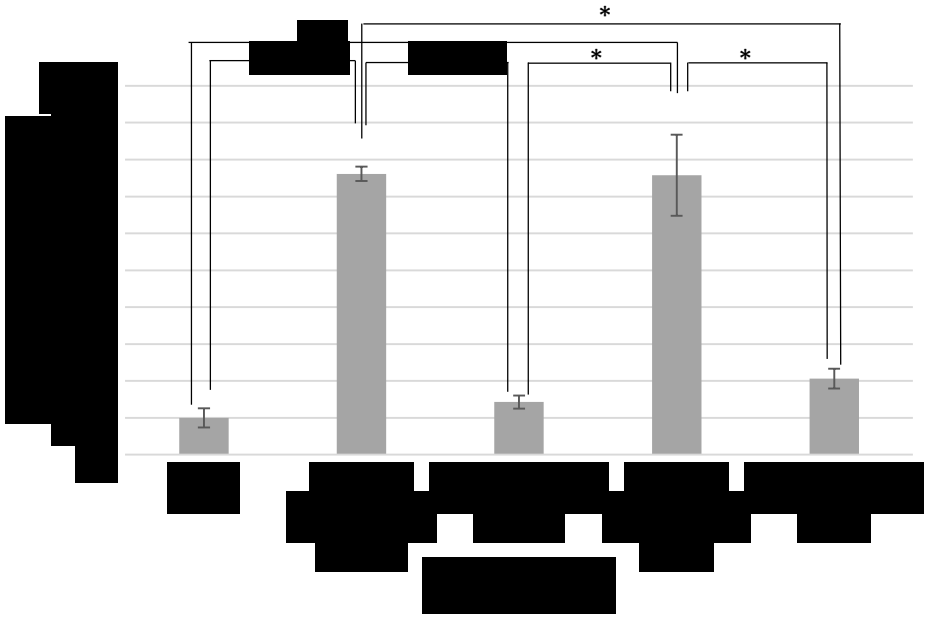

Fig.7. Activation of PAI-1 promoter by fractionated human volunteer serum (100kDa)

PAI-1 clone 8 HK-2 cells were exposed to SFM, 0.5% or 1% of 100kDa fractions of human volunteer serum. Media and cells were harvested at 24h. The luciferase activity was measured using the end point luciferase assay method and the data was normalised to total cellular protein in each well. The data are presented as a percentage of the control value (SFM exposure) which was 119,000,000 RLU. (n=4, *p≤0.05).

To verify the 100kDa fractionation results, serum from another volunteer was fractionated following the same protocol as above. The cells were exposed to SFM treated with either 0% serum, 1% whole serum, 1% >100kDa concentrate or 1% <100kDa filtrate for 24 hours.

The results were similar to the data shown in Figure 5: the >100kDa concentrate fraction caused a significant increase in PAI-1 promoter activity in comparison to the filtrate fraction (Figure 8). Furthermore, the whole serum tested in this assay demonstrated reduced ability to activate the PAI-1 promoter in comparison to the >100kDa concentrate fraction.

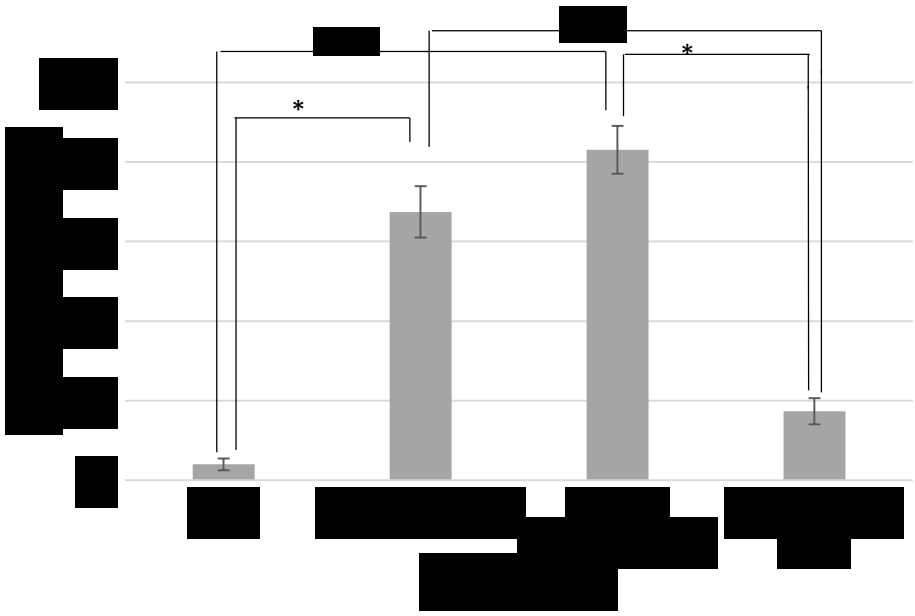

Fig.8. Activation of PAI-1 promoter by whole and 100kDa filtrated human serum

PAI-1 clone 8 cells were exposed for 24h to 1% of fractionated or whole serum from a volunteer. The luciferase activity was measured using the end point luciferase assay method and the data were normalised to total cellular protein in each well. The data are presented as a percentage of the control value (SFM) that was 19,500,000 RLU. (n=4, *p≤0.05).

3.2 PAI-1 Reporter gene assay in response to 50kDa fractionated human serum

To further fractionate serum proteins according to their size, a 50kDa vivaspin 2 ultracentrifuge tube was used to produce >50kDa concentrate or <50kDa filtrate fractions. PAI-1 clone 8 HK-2 cells were exposed for 24 hours to SFM, 1% whole serum, 1% >50kDa concentrate or 1% <50kDa filtrate fractions.

The serum fractions produced a similar effect to the 100kDa fractionation assays with the >50kDa concentrate causing a significant increase in PAI-1 promoter activity when compared to the <50kDa filtrate fractions (Figure 9). In contrast to the results shown in Figure 8, the effect of the >50kDa concentrate fraction was lower than the effect of the whole serum.

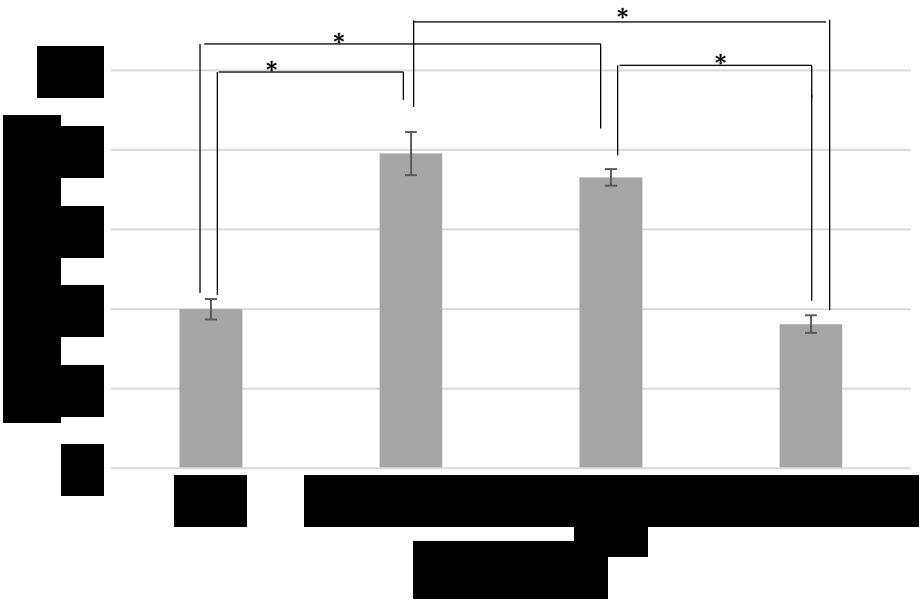

Fig.9. Activation of PAI-1 promoter by 50kDa filtrated human serum

PAI-1 clone 8 HK-2 cells were exposed to SFM, 1% of fractionated or whole human volunteer serum. Media and cells were harvested at 24h. The luciferase activity was measured using the end point luciferase assay method and the data were normalised to total cellular protein in each well. The data is presented as a percentage of the control value (SFM) that was 1,125,000,000 RLU. (n=4, *p≤0.05).

3.3 SDS-PAGE and silver staining of human serum fractions

Silver staining of SDS-PA gels was carried out to examine the protein composition of the different serum fractions. The silver staining demonstrated that the 50 kDa and 100 kDa concentrate fractions contained a protein band of approximately 29kDa with intensity similar to that in the whole serum (Figure 10). Furthermore, the 50 kDa filtrate fraction contained traces of proteins with molecular size greater than >60 kDa but did not display the presence of the 29 kDa band. Similarly, the 100 kDa filtrate contained protein bands with molecular size greater than 100 kDa but did not contain the 29 kDa protein.

These results suggested that the filtration method chosen to fractionate serum was ineffective and all further experiments were carried out using whole serum.

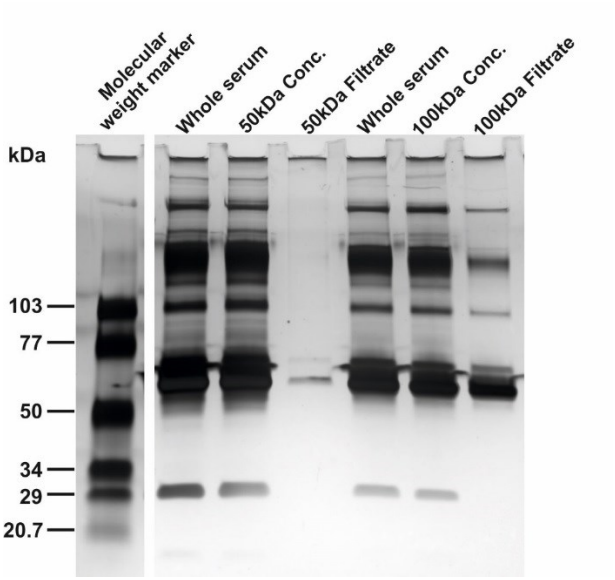

Fig.10. Silver stain SDS-PAGE of human serum fractions

Serum fractions or whole serum (1µg of total protein) were loaded onto a 4-15% continuous gradient gel and subjected to SDS-PAGE and silver staining.

3.4 PAI-1 Reporter gene assay in response to whole and heat-inactivated human serum

To evaluate the effect of the complement on the activation of PAI-1 promoter, heat-inactivated and the respective native human sera were incubated with PAI-1 clone 8 HK-2 cells and the secretion of luciferase in the m medium was measured. Whole serum was heated at and then mixed with SFM to produce 0.5% inactivated human serum treated media.

Heat inactivation of the serum caused a reduction in PAI-1 promoter activity by two fold when compared to native serum (Figure 11A). This indicated that the complement or other pro-fibrotic factors degraded during the heat-inactivation can up-regulate PAI-1 expression.

To visualise the integrity of the proteins in native and heat-inactivated sera, samples were separated on SDS-PA gels and the proteins were visualised using silver staining (Figure 11B). The results demonstrated no difference in the pattern of major serum proteins between native and heat-inactivated serum.

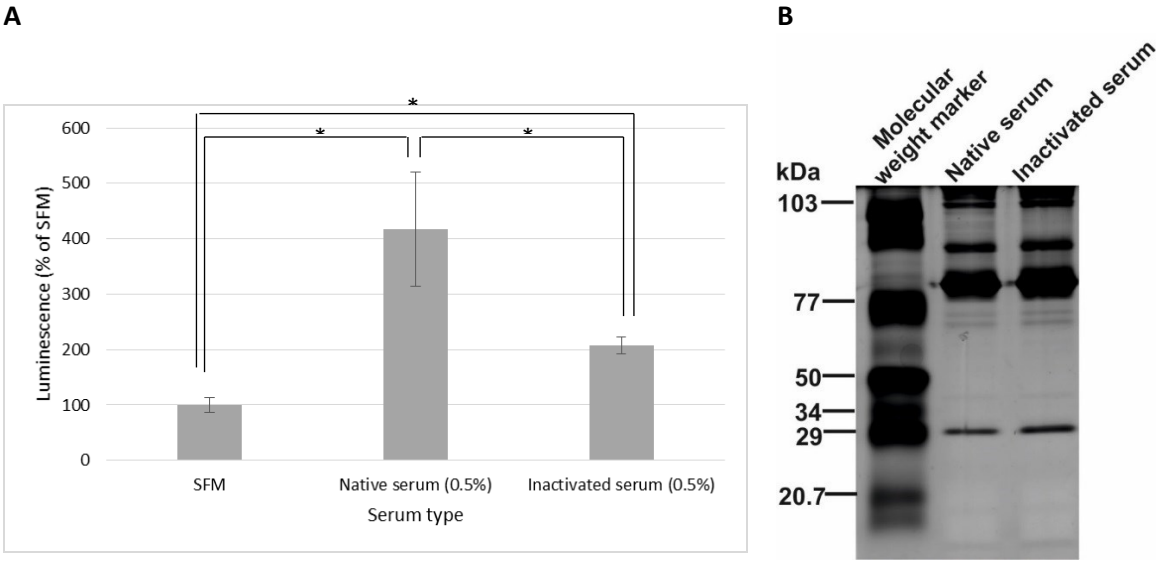

Fig.11. PAI-1 promoter activation (A) and silver stained SDS-PA gel of native and heat-inactivated human sera (B)

A: PAI-1 clone 8 cells were grown to 80% confluency in a 24 well plate, growth arrested for 24 in SFM and washed prior exposure to eithier 0.5% native or 0.5% heat inactivated serum (56°C for 30 minutes). Media and cells were harvested at 24h. Luciferase activity was measured using the end point luciferase assay method with the coelenterazine substrate and the data were normalised to total cellular protein in each well. The data is presented as a percentage of the control value, which in this assay was the 0% value that was 1,241,325 RLU. (n=4, *p≤0.05).

B: 1µg of native or heat-inactivated serum were separated on a 12% discontinuous gel and protein bands were detected using a silver staining methods.

3.5 Western blot of HK-2 cells exposed to native and inactivated human serum

Western blotting was carried out to evaluate the levels of PAI-1 protein expressed by HK-2 cells exposed for 24 hours to SFM, 0.5% or 1% native or inactivated serum (Figure 12a). Densitometry of the bands demonstrated an increased PAI-1 expression in response to 1% native and inactivated human serum in comparison with cells exposed to SFM (Figure 12B).

Based on these results, native, non-fractionated sera were used in all further experiments.

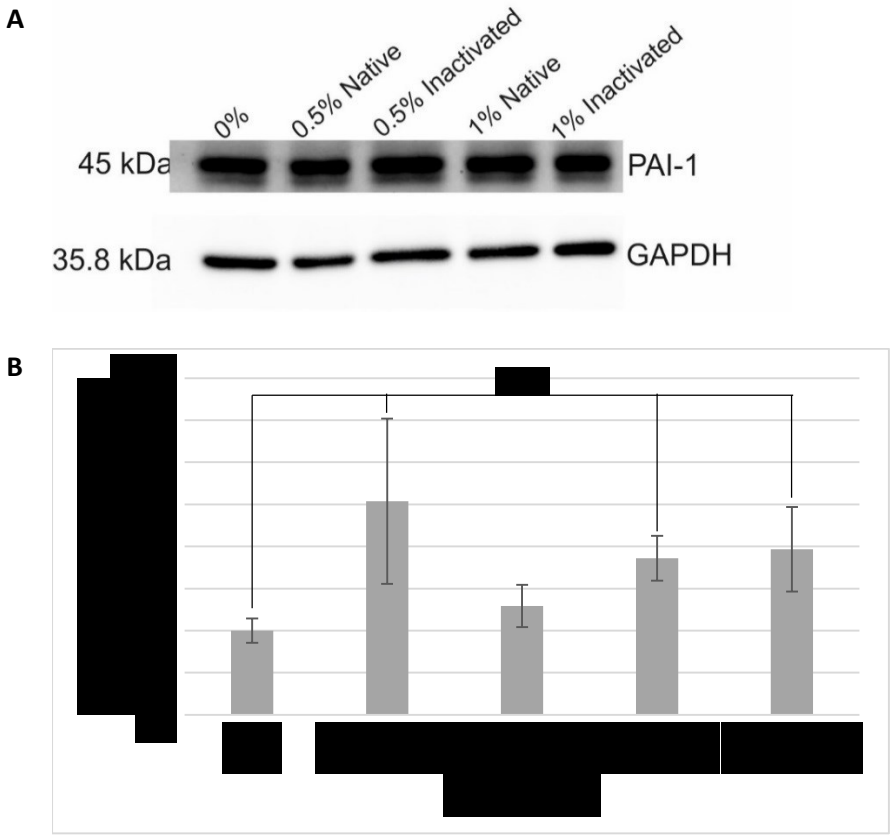

Fig.12. Expression of PAI-1 in HK-2 cells exposed to native or heat-inactivated serum

Cells were harvested using RIPA buffer, sonicated and 10µg of total protein were loaded per SDS-PAG well. Nitrocellulose membranes were exposed to antibodies for PAI-1 and GAPDH **(A)**. The intensity of each band was measured using densitometry and the expression of PAI-1 was normalised to GAPDH band intensity **(B)**. The data were presented as a percentage of the control value (cells exposed to SFM (0%)) (n=2, *p≤0.05 vs. 0%)

3.6 Viability assay of HK-2 cells exposed to serum

HK-2 cells were grown to 80% confluency and then exposed to SFM, or 1% of either volunteer or patient sera (stage 3a, 3b, 4 or 5) for 24 h (Figure 13A) or 48 hours (Figure 13B).

The results suggest that there is an increase viability in the presence of serum as compared to cells exposed to SFM. This effect could result from increased cell numbers (proliferation) in response to growth factors in the sera. However, it appears that increasing CKD stage impairs the viability of the cells, as compared to volunteer samples. The most profound effect was observed in particular with sera from patients with CKD stage 4 and stage 5.

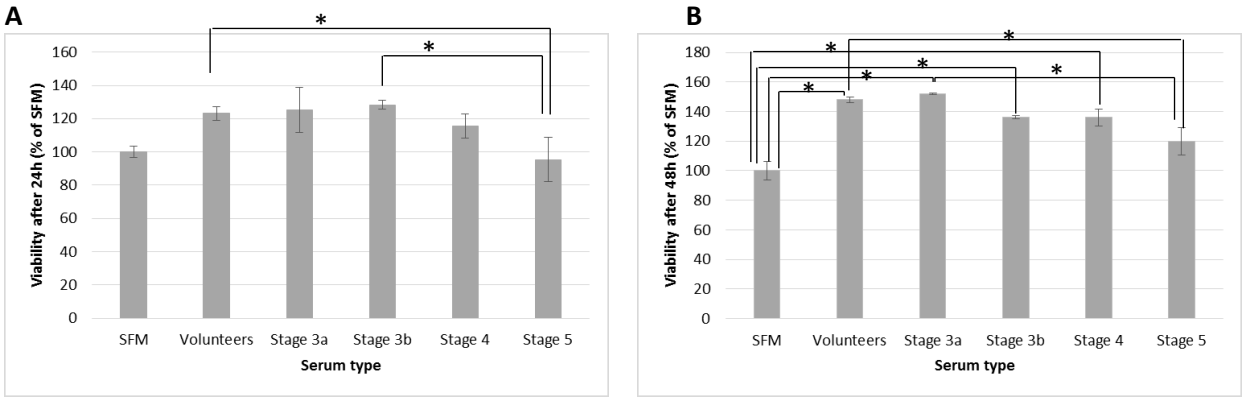

Fig.13. Viability of HK-2 cells exposed to SFM, volunteer or patient sera

The viability was estimated in cells grown in 96 well plates at 24h **(A)** and 48h **(B)** by measuring the accumulation of the highly water-soluble tetrazolium salt WST-8 in the medium. The data are presented as a percentage of the viability of cells exposed to SFM (n=4, *p≤0.05).

3.7 PAI-1 Reporter gene assay in response to CKD patient serum

PAI-1-pNL2.3 clone 8 cells were exposed for up to 48 hours to SFM, 1% of each of the 16 CKD patient sera or 1% of 7 healthy volunteer sera. Media were harvested at 4h, 24h, 30h and 48h and luciferase activity was measured using the time course luciferase assay method.

The exposure of the volunteer and patient serum significantly increased the luciferase secretion compared to the SFM but there was no significant difference observed between the volunteer serum and any stage of CKD patient serum throughout the time course.

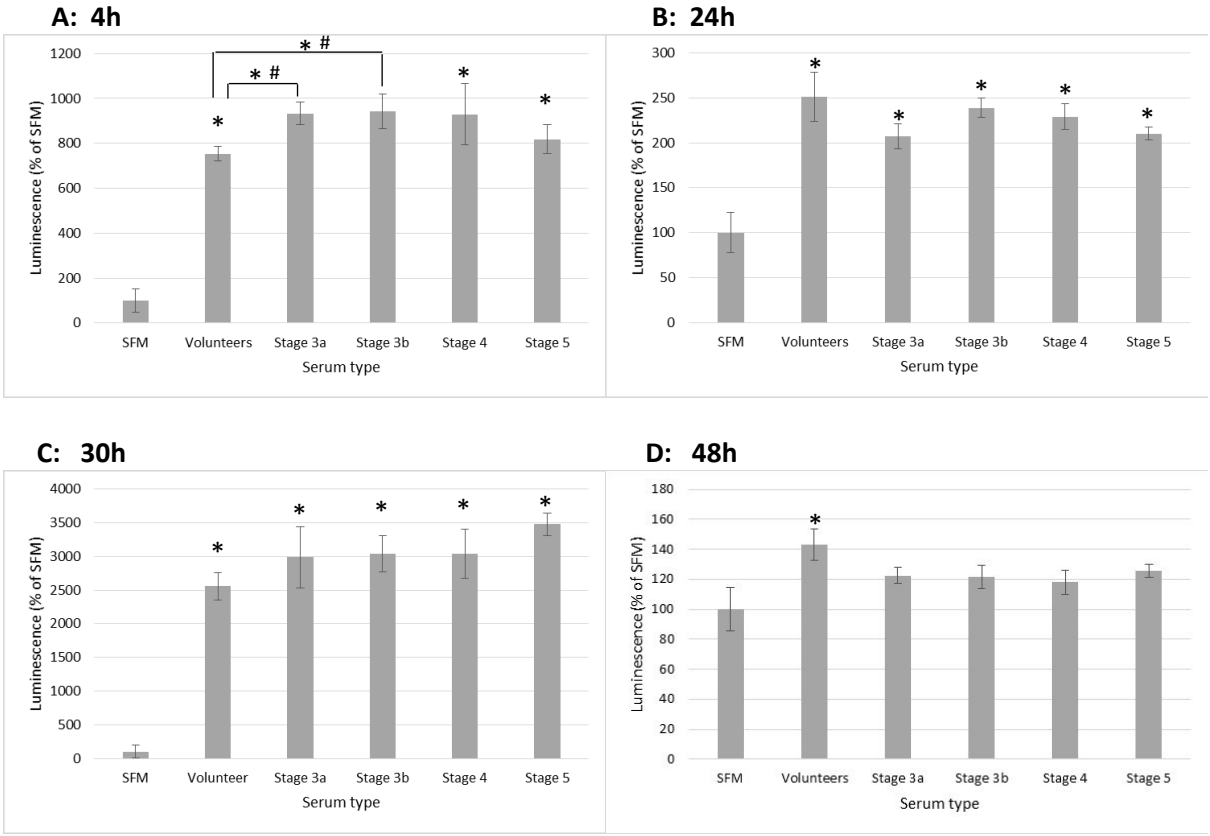

Fig.14. Activation of PAI-1 promoter by CKD patient serum over 48h

Activation of PAI-1 promoter by CKD patient serum after **A)** 4 hours, **B)** 24 hours, **C)** 30 hours, **D)** 48 hours. PAI-1 clone 8 HK-2 cells were exposed to either healthy volunteer or CKD patient human serum of either stage 3a, 3b, 4 or 5. Media were harvested at 4h, 24h, 30h and 48h. The luciferase activity was measured using the time-course luciferase assay method with the coelenterazine substrate and the data was normalised to total protein content in each well. The data were presented as a percentage of the control value (SFM) (n=4. *p≤0.05 vs. SFM; #p≤0.05 vs. SFM, stage 3a, 3b, 4 and 5)

3.8 Expression of markers of fibrosis in response to CKD patient serum

The effect of volunteer and patient sera on the protein expression of the markers of fibrosis was studied using Western blot. Figure 15 shows the intensity of PAI-1 and collagen 1 bands after exposure to SFM, volunteer or patient sera (Stage 3a, 3b, 4 and 5) for 24h or 48h.

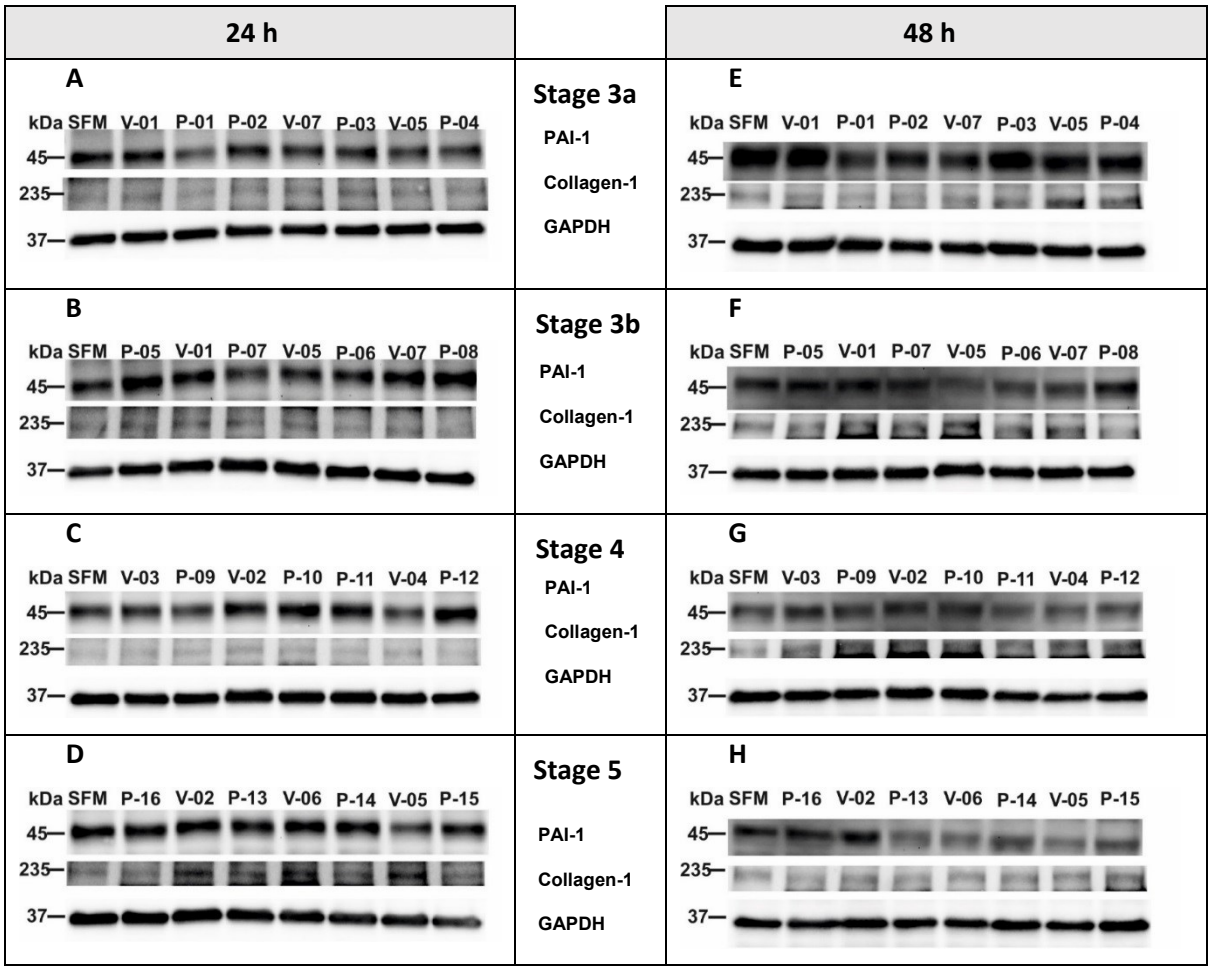

Fig.15. Western blot image and expression graphs of HK-2 cells exposed to Volunteer and CKD patient sera

Western blot images PAI-1, collagen 1 and GAPDH levels in HK-2 cells exposed to volunteer sera and **A)** stage 3a CKD patient sera (24h; **B)** stage 3b CKD patient sera (24h), **C)** stage 4 CKD patient sera (24h), **D)** stage 5 CKD patient sera (24h), **E)** stage 3a CKD patient sera (48h), **F)** stage 3b CKD patient sera (48h), **G)** stage 4 CKD patient sera (48h), **H)** stage 5 CKD patient sera (48h). HK-2 cells were grown in 6 well plates and were exposed to SFM or 1% of either volunteer or patient sera (CKD 3a, 3b, 4 or 5) for either 24 or 48 hours. 30µg of total protein were loaded into 4-15% continuous gradient gels with volunteer and patient sera being matched by age and sex (n=2).

The results of densitometry analysis of the target bands (Figure 16) show that after 24 h of exposure to sera, the level of PAI-1 expression increases with the progressive CKD stages, reaching a maximum at stage 4 of CKD (Figure 16A). In contrast, sera from patients with stage 5 CKD demonstrated reduced levels of PAI-1. Similar pattern of expression was observed in cells exposed to sera for 48 h (Figure 16C).

Although the magnitude of change was lower, the pattern of collagen-1 expression mimicked the pattern for PAI-1, both at 24h and 48h (Figure 16B and D). Interestingly, the collagen-1 levels in response to exposure for 48 h to sera from patients with CKD stage 4 were significantly higher in comparison with volunteer or patient sera.

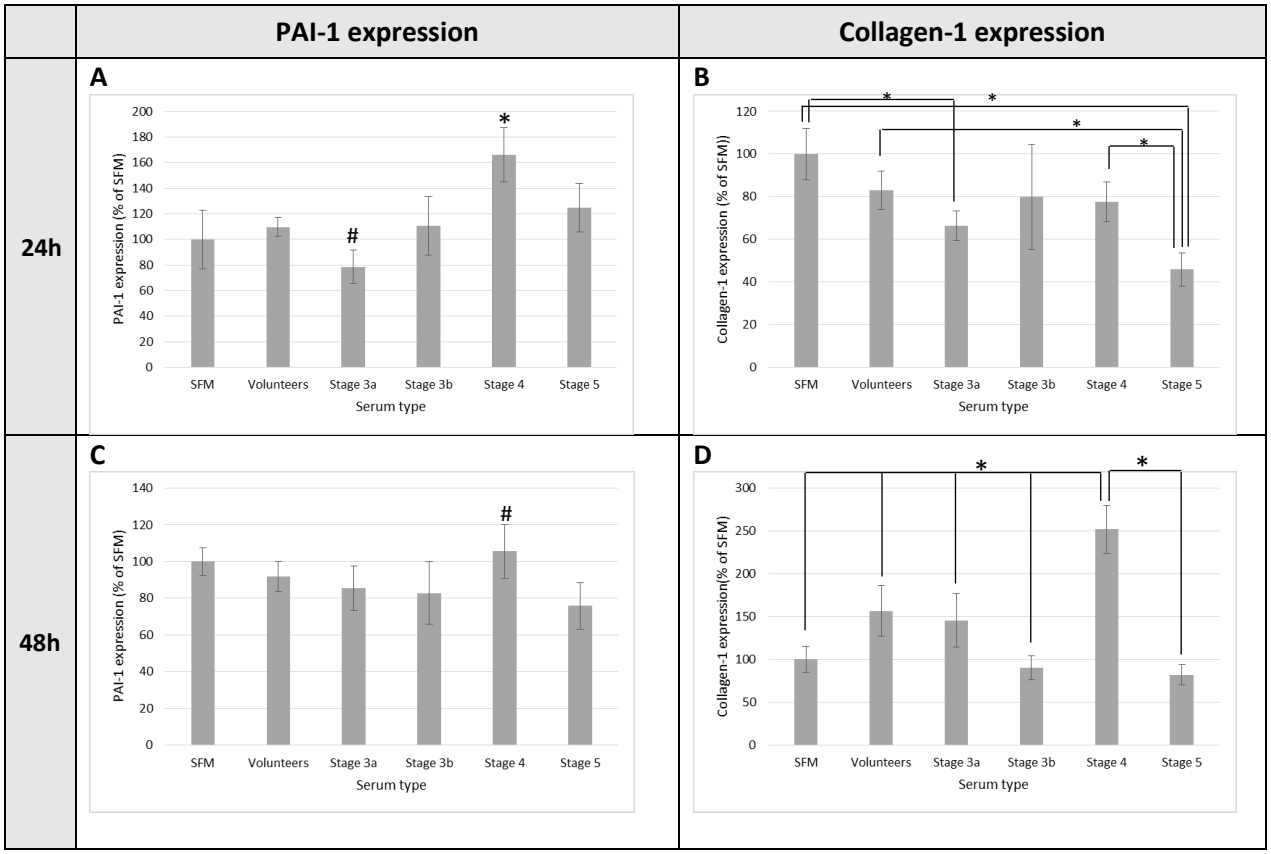

Fig.16. PAI-1 and Collagen-1 expression in response to 24 or 48h exposure to volunteer or patient sera

Densitometry analysis of PAI-1, collagen-1 and GAPDH protein expression in response to volunteer and patient sera as detected by Western blotting: **A)** PAI-1 after 24h**, B)** Collagen-1 after 24h**, C)** PAI-1 after 48h, **D)** Collagen-1 after 48h. The intensity of each band was measured using ImageLab software and the expression of PAI-1 and Collagen-1 was normalised to the respective GAPDH levels. The data are presented as a percentage of the control value (SFM), (*p≤0.05 vs. SFM, volunteers, stage 3a, 3b and 5; #p≤0.05 vs. stage 5; n=4)

3.9 miRNA analysis of HK-2 cells exposed to CKD patient serum

HK-2 cells were exposed for 24 or 48 hours to SFM or 1% of either volunteer or CKD patient serum (stage 3a, 3b, 4 or 5). Total RNA was isolated, reverse transcribed to complementary DNA (cDNA) and qPCR fibrosis arrays were carried out to measure changes in miRNA levels of 84 fibrosis-related miRNAs.

3.9.1 Scatter plots of miRNA up and down regulation in CKD patient serum exposed cells when compared to volunteer serum

The fibrosis-related miRNAs fold-increase in response to exposure of HK-2 cells to patient sera of different CKD stage when compared to volunteer sera are presented as scatter plots in Figure 15.

Six miRNAs were upregulated and 5 miRNAs were downregulated after 24 hours in CKD stage 3a when compared to the volunteer sera (Figure 17A). When results from exposure to stage 3b sera was analysed, there were 15 upregulated miRNAs but only 1 downregulated (Figure 17B). For stages 4 and 5 (figures 17C and 17D) there were 8 and 7 upregulated miRNAs respectively when compared to the effect of volunteer sera, and for both stages there were 4 miRNAs downregulated.

After 48 hours the numbers of miRNAs upregulated by patient vs. the volunteer sera were generally lower. For stage 3a, 3b, 4 and 5 there were 5, 6, 9, and 5 upregulated miRNAs respectively. For downregulated miRNAs the numbers were 4, 2, 3, and 4, respectively.

Tables 8 and 9 list the miRNAs that demonstrated a significant upregulation or downregulation (above or below factor of 2) after 24 hours or 48 hours respectively, as compared to HK-2 cells exposed to volunteer sera.

When comparing the 24 and 48 hour miRNA expression across the stages it appears as though more miRNAs were expressed after 24 hours rather than after 48 hours.

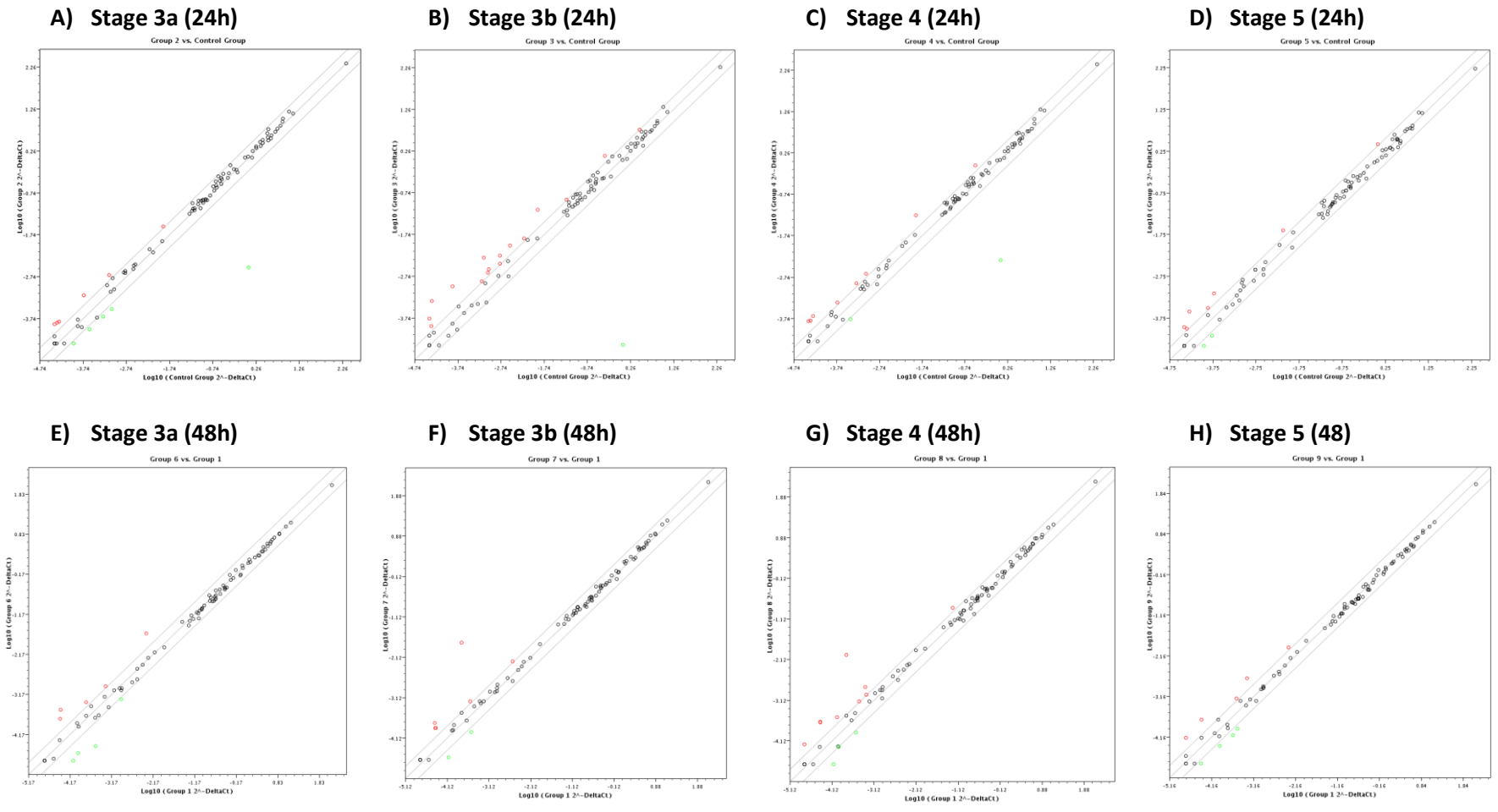

Fig.17. Scatter plots showing fold increase or decrease of individual fibrosis related miRNAs of CKD patients compared to volunteers

Scatter plots of miRNA expression after 24h exposure of HK-2 cells to CKD patient sera as compared to volunteer sera: stage 3a **(A);** stage 3b **(B)**; stage 4 **(C);** stage 5 **(D)** or after 48h exposure to CKD patient sera as compared to volunteer sera: stage 3a **(E);** stage 3b **(F)**; stage 4 **(G);** stage 5 **(H).** The data analysis was carried out using StepOnePlus™ software v2.3 and the miScript miRNA PCR Array Data Analysis program (SabioSciences).

Table.8. Fold increase and decrease of fibrosis-related miRNA in HK-2 cells exposed for 24h to 1% serum from CKD patients, as compared to miRNA expression in HK-2 cells exposed to volunteer sera

	miRNA Upregulation				miRNA Downregulation			
miRNA	**Stage 3a**	**Stage 3b**	**Stage 4**	**Stage 5**	**Stage 3a**	**Stage 3b**	**Stage 4**	**Stage 5**
hsa-miR-101-3p	-	2.064	-	-	-	-	-	-
hsa-miR-122-5p	3.427	-	2.321	3.696	-	-	-	-
hsa-miR-129-5p	-	2.155	-	-	-	-	-	-
hsa-miR-150-5p	-	7.718	-	2.276	-	-	-	-
hsa-miR-18a-5p	-	-	2.797	-	-	-	-	-
hsa-miR-199a-5p	-	-	-	-	-2.478	-	-	-
hsa-miR-199b-5p	-	-	-	-	-2.691	-	-	-
hsa-miR-204-5p	-	2.639	-	-	-	-	-	-
hsa-miR-208a-3p	-	-	3.993	-	-	-	-	-
hsa-miR-216a-5p	-	-	-	-	-	-	-	-2.554
hsa-miR-217	-	-	-	2.164	-403.6	-29185	-260.1	-
hsa-miR-223-3p	3.424	4.519	-	2.744	-	-	-	-
hsa-miR-31-5p	-	3.001	-	-	-	-	-	-
hsa-miR-32-5p	-	2.110	-	-	-	-	-	-
hsa-miR-335-5p	-	2.885	-	-	-	-	-	-
hsa-miR-338-5p	2.730	7.089	-	-	-	-	-	-
hsa-miR-372-3p	-	-	-	-	-2.358	-	-	-2.891
hsa-miR-375	-	2.514	2.482	-	-	-	-	-
hsa-miR-377-3p	3.050	-	4.152	5.029	-	-	-	-
hsa-miR-382-5p	-	2.365	-	-	-	-	-	-
hsa-miR-449a	-	3.338	-	-	-	-	-	-
hsa-miR-449b-5p	3.219	10.529	3.643	2.250	-	-	-	-
hsa-miR-451a	-	-	-	-	-	-	-2.183	-
hsa-miR-491-5p	2.193	5.463	4.337	-	-	-	-	-
hsa-miR-5011-5p	-	3.302	-	-	-	-	-	-
hsa-miR-5692a	-	-	2.482	-	-2.587	-	-	-
hsa-miR-874-3p	-	-	-	2.986	-	-	-	-

Table 9. Fold increase and decrease of fibrosis-related miRNA in HK-2 cells exposed for 48h to 1% serum from CKD patients, as compared to miRNA expression in HK-2 cells exposed to volunteer sera

	miRNA Upregulation				miRNA Downregulation			
miRNA	**Stage 3a**	**Stage 3b**	**Stage 4**	**Stage 5**	**Stage 3a**	**Stage 3b**	**Stage 4**	**Stage 5**
hsa-miR-122-5p	7.106	3.351	5.619	-	-	-	-	-
hsa-miR-129-5p	-	-	3.468	-	-	-	-	-
hsa-miR-150-5p	-	-	-	-	-8.224	-2.638	-2.335	-2.565
hsa-miR-199a-5p	-	-	-	-	-	-	-	-2.915
hsa-miR-199b-5p	2.246	-	2.135	3.980	-	-	-	-
hsa-miR-208a-3p	-	-	3.681	3.980	-	-	-	-
hsa-miR-211-5p	-	4.659	-	-	-	-	-	-2.507
hsa-miR-215-5p	-	-	-	-	-2.275	-	-	-
hsa-miR-216a-5p	-	-	2.933	-	-	-	-	-
hsa-miR-217	-	104.89	59.811	-	-	-	-	-
hsa-miR-223-3p	-	-	-	-	-4.453	-	-	-
hsa-miR-325	-	-	-	-	-	-	-2.005	-2.617
hsa-miR-372-3p	-	-	-	-	-5.396	-3.171	-4.028	-
hsa-miR-377-3p	-	-	2.111	-	-	-	-	-
hsa-miR-449a	-	2.167	-	-	-	-	-	-
hsa-miR-449b-5p	4.229	3.441	5.444	4.736	-	-	-	-
hsa-miR-451a	2.643	-	-	-	-	-	-	-
hsa-miR-5692a	-	2.281	-	2.282	-	-	-	-
hsa-miR-663a	-	-	2.515	-	-	-	-	-
hsa-miR-874-3p	4.806	-	-	2.390	-	-	-	-

3.9.2 Summary of the miRNA expression data after 24h or 48h of treatment with patient sera

The miRNAs listed in Tables 8 and 9 are presented in Venn diagrams to facilitate the analysis of the pattern of miRNA regulation in relation to CKD stage (Figure 18). The miRNAs in the array kit are grouped in 7 categories depending on their function: Pro-Fibrotic, Anti-Fibrotic, Extracellular Matrix Remodelling & Cell Adhesion, Inflammation, Angiogenesis, Signal Transduction and Transcriptional Regulation and Epithelial-to-Mesenchymal Transition (Appendix 2).

A comparison of the miRNAs upregulated after 24 h and 48 h of exposure to patient sera (Figure 18A and 18C) reveals that the Anti-Fibrotic miR-449b-5p was the only miRNA that was upregulated by sera of all CKD stages. Not a single common miRNA was down-regulated by exposure to sera of all CKD stages after 24 and 48h (figures 18B and 18D). However, miR-217 was strongly down-regulated after 24h, more so than any other miRNA so it is likely that miR-217 plays an essential role in fibrosis, according to appendix 2 miR-217 is related to both Extracellular Matrix Remodelling & Cell Adhesion and Signal Transduction and Transcriptional Regulation.

CKD stage 3a sera affected 5 miRNAs related to Pro-fibrosis (miR-199b, 338, 377, 5692a, 215), 1 related to Anti-fibrosis (miR-449b), 4 related to Extracellular Matrix Remodelling & Cell Adhesion (miR-199a, 199b, 217, 451a), 2 related to inflammation (miR-122 and 199a), 2 related to angiogenesis (miR-372 and 150), 6 related to Signal Transduction & Transcriptional Regulation (miR-122, 217, 223, 372, 491, 451a), and 4 related to Epithelial-to-Mesenchymal Transition (miR-199a, 199b, 215, 874).

CKD stage 3b affected 5 miRNAs related to Pro-fibrosis (miR-338, 32, 382, 5011, 5692), 5 related to Anti-fibrosis (miR-449b, 204, 335, 449a, 211), 3 related to Extracellular Matrix Remodelling & Cell Adhesion (miR-217, 204, 449a), 3 related to inflammation (miR-129, 204, 122), 5 related to angiogenesis (miR-150, 10, 31, 375, 372), 8 related to Signal Transduction & Transcriptional Regulation (miR-217, 223, 491, 101, 204, 449a, 122, 372) and 1 related to Epithelial-to-Mesenchymal Transition (miR-382).

CKD stage 4 affected 5 miRNAs related to Pro-fibrosis (miR-377, 5692, 208a, 216a, 199b), 3 related to Anti-fibrosis (miR-449b, 199b, 18a), 2 related to Extracellular Matrix Remodelling & Cell Adhesion (miR-217 and 451a), 2 related to inflammation (miR-122 and 129), 3 related to angiogenesis (miR-150, 375, 372), 7 related to Signal Transduction & Transcriptional Regulation (miR-122, 217, 491, 18a, 451a, 372, 663a) and 2 related to Epithelial-to-Mesenchymal Transition (miR-199b and 325).

CKD stage 5 affected 5 miRNAs related to Pro-fibrosis (miR-377, 208a, 216a, 5692, 199b), 2 related to Anti-fibrosis (miR-449b and 211), 3 related to Extracellular Matrix Remodelling & Cell Adhesion (miR-217, 199a, 199b), 2 related to inflammation (miR-122 and 199a), 2 related to angiogenesis (miR-372 and 150), 4 related to Signal Transduction & Transcriptional Regulation (miR-122, 217, 223, 372) and 4 related to Epithelial-to-Mesenchymal Transition (miR-874, 199a, 199b, 325).

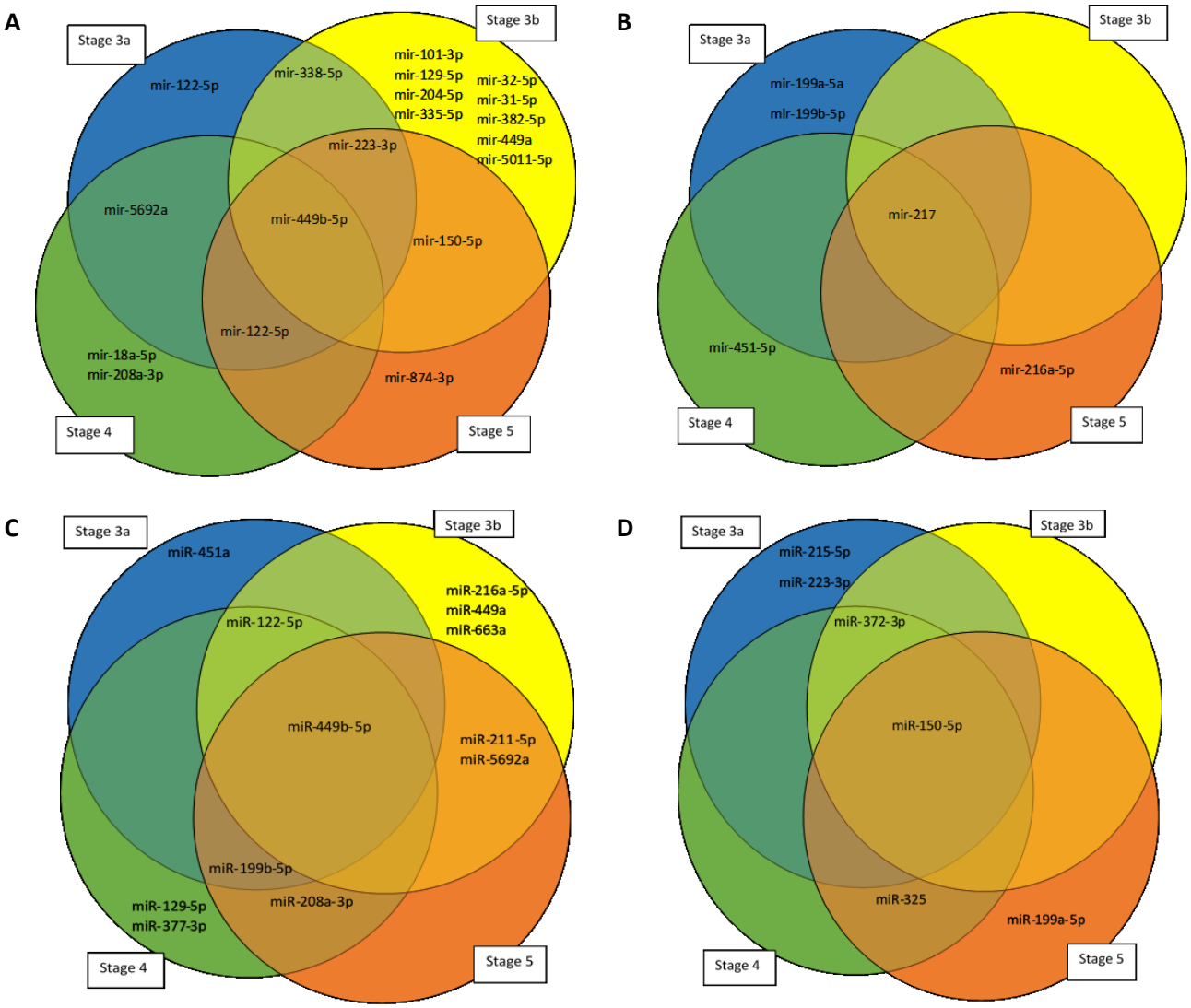

Fig.18. Venn diagrams by CKD stage of miRNAs up- or down-regulated after 24h or 48h of exposure to CKD patient sera

A) Up-regulated miRNA species after 24h incubation with patient sera; **B)** Down-regulated miRNA species after 24h incubation with patient sera; **C)** Up-regulated miRNA species after 48h incubation with patient sera; **D)** Down-regulated miRNA species after 48h incubation with patient sera

4 Discussion

The aim of this this study was to identify novel fibrosis-related miRNA targets for treatment of CKD by exposing RPTEC to sera of patients with different stages of diabetic nephropathy (DN). In healthy kidneys, proteins of molecular weight smaller than 40-50 kDa are filtered freely in the primary urine whereas proteins with molecular size >100 kDa are almost completely excluded from the filtrate (Ruggiero et al., 2010). In health, the majority of the filtered proteins are reabsorbed by the proximal tubules. However, the progression of diabetic nephropathy is often associated with increased proteinuria (Jefferson et al.), which is an end result of increased protein filtration in the glomerulus and decreased reabsorption of the filtered proteins by the proximal tubules. Recently it was demonstrated that patients with DN without proteinuria show similar histological renal damage as patients with proteinuria (Caramori et al., 2003). This suggests that molecular factors other than protein may exacerbate renal damage (e.g. through TIF) in DN.

4.1 Fractionation and inactivation of human serum

To investigate whether serum fractions containing proteins of different molecular size have a different effect on markers of fibrosis in human RPTEC depending on the stage of kidney disease, an initial objective of this study was to separate serum into fractions of defined molecular sizes using commercially available filtering devices, and to investigate the ability of each fraction to up-regulate markers of fibrosis. However, the results demonstrated that the chosen devices with cut-offs of 100kDa and 50kDa were unable to yield protein fractions with the expected molecular sizes, as demonstrated by silver gel staining. The presence in the concentrate of protein bands of significantly lower molecular weight than the membrane cut-off but not in the filtrate suggests that that the membranes of the devices may have been clogged by the excessive amounts of protein in the whole serum. Due to the lack of reasonable fractionation alternatives, all further experiments were carried out with whole serum.

To test whether complement activation plays a significant role on the expression of markers of fibrosis (e.g. PAI-1), heat inactivated human sera and native human sera were compared. The results indicated that the heat inactivation, which leads to deactivation of the complement, decreased the PAI-1 promoter activation and PAI-1 protein expression. It has been shown that in macrophages the anaphylatoxin C5a complement fragment can induce the expression of PAI-1 via Nuclear Factor-κB (NF-κB) activation (Kasti et al., 2006). Therefore, the moderate decrease in PAI-1 promoter activation and protein expression by inactivated serum may be due to the inability to form C5a fragment or to the degradation of key protein factors. Therefore, native whole serum was used in all further experiments.

4.2 Viability of HK-2 cells exposed to human sera

The kit used to measures viability in this study utilises the formation of soluble formazan dye produced by dehydrogenases in cells and therefore, reflects the number of living cells. The stepwise decrease of cell viability in response to sera from patients with increasing stage of CKD suggests the gradual accumulation of toxic or anti-proliferative factors with renal disease. The viability was lowest in response to sera from stage 5 CKD patients, especially after 48h, suggesting accumulation of such factors due to minimal renal function.

The percentage of serum used in the experiments (1%) does not seem to cause an issue to the cells as the viability in response to stage 3a sera is very similar to the response to volunteer sera, and is significantly higher than of cells exposed to SFM. Research has shown that the later stages of CKD are associated with reduced viability in renal proximal tubular cells, as CKD stages 4 and 5 lead to increased levels of p-cresol (Huang et al., 2012) which induces oxidative stress within the cells, this leads to increased autophagic cell death and decreased viability in the cells (Lin et al., 2015).

4.3 Activation of PAI-1 promoter by serum from DN patients and healthy volunteers

Verification of the functionality of the PAI-1 promoter construct using transfected HK-2 cells that were exposed to acidosis demonstrated that within 24h period there was a stepwise increase in luciferase activity, which was significantly increased by acidosis. These data confirmed results from previous research in our group showing a significant increase in PAI-1 protein expression after a 24 h exposure to acidosis (2.5 fold) compared to cells exposed to pH 7.4, as detected by Western blot (data not shown). These results are supported by data showing that acidosis increases PAI-1 expression in mesothelial cells (Bergstrom et al., 2006). Furthermore, acidity appears to increase the stability and half-life of PAI-1 from 2h (physiological conditions) to 8h (pH 6.5) (Yildiz et al., 2014).

Although an increase of the PAI-1 promoter activation was observed over the following 24-48h of exposure, exposure to pH 6.7 have resulted in reduced PAI-1 promoter activation, reflecting adaptive changes in the cells (data not shown).

These results suggested that the PAI-1 promoter construct is functional and therefore it was used in further experiments to determine the time-course of reactivity to human sera.

The luciferase expression of the CKD stage 3a and 3b samples are significantly higher than the volunteer samples after 4 hours implying that the patient serum does increase PAI-1 production. However, this is contradicted by the results for CKD stage 5 as while it is not significantly different to the other stages it does appear to be lower. This could be supporting the theory that the stage 5 patients were undergoing dialysis and the serum sample was taken post-dialysis which would reduce the levels of CKD related serum factors within the serum. Further research would need to take place with the knowledge at which point the serum was taken from the patient.

The PAI-1 expression levels of all CKD stages samples after 24 and 48 hours are reduced with the volunteer's serum showing the same or higher expression levels as after 4 hours. This implies that after 4 hours the increased PAI-1 expression caused by the CKD serum returned to basal level which is supported by research showing similar effects where PAI-1 expression peaked at 4 hours then dropped after (Suzuki et al., 2002).

4.4 Protein expression of PAI-1 and Collagen 1 in HK-2 cells exposed to human sera

The protein expression PAI-1 of HK-2 cells exposed to sera varied between CKD stages, with no significant change induced by CKD stage 3a, 3b and 5 as compared to the volunteer samples at 24h and 48h. However, in response to stage 4 serum, PAI-1 expression was significantly higher than all other treatments at 24h, and moderately increased after 48h of exposure. The expression of PAI-1 levels in the different CKD stages is not well documented but in other research it has been observed that the TGF-β levels are increased in the advanced stages of CKD (August and Suthanthiran, 2003) which as discussed is involved in the activation of PAI-1. Interestingly, after a 24h exposure to patient

or volunteer sera, the collagen-1 levels were significantly decreased in comparison to cells exposed to SFM. However, after 48h a significant increase of collagen-1 protein was observed in cells exposed to stage 4 CKD sera. This may be a delayed response to the increased PAI-1 protein at 24h.

The protein levels of PAI-1 and collagen 1 in response to stage 5 CKD sera at 24h and 48h of exposure were lower than to stage 4 sera, thus providing further evidence for the presence of cytotoxic/anti-proliferative factors at this stage.

Between the PAI-1 and Collagen-1 expression it appears that CKD stage 4 is when the expression of PAI-1 increases leading to the production of Collagen after 48 hours and contributing heavily to the accumulation of ECM and the progression of TIF (Ghosh and Vaughan, 2012).

4.5 Fibrosis related miRNA expression in response to human serum

When comparing the miRNAs expression at 24h or 48h in response to sera from DN patients with different stages of CKD to sera from healthy volunteers, some interesting results were observed: for example, miR-449b was the only miRNA upregulated by patient sera of every CKD stage both at 24 and 48h. Furthermore, miR-217 was down-regulated by sera of all CKD stages after 24h but not after 48h. When comparing the expression of the fibrosis related miRNAs between the 24 hour volunteer samples and the 48 hour volunteer samples (data not shown) the expression of miR-217 was downregulated in the 48 hour volunteer samples by over 7000 fold. This means that while the miR-217 expression in 48 hour patient samples may appear to be either normal or slightly upregulated they would still be severely down-regulated when compared to the 24 h volunteers.

Overall, the expression of 31 miRNAs was dysregulated after 24h and 48h incubation with the patents sera. As the aim of this project was to identify potential therapeutic targets for preventing the progression of CKD in diabetic nephropathy, below are listed a selection of miRNAs dysregulated by sera from patients with CKD stage 3a (12 miRNAs overall), which are of interest for further investigation.

4.5.1 Up-regulated miRNAs after 24 h and 48 h exposure to human sera

miR-449b

miR-449b is described as an anti-fibrotic miRNA in the Qiagen's miRNA array manual. miR-449b has been shown to inhibit cell proliferation and migration, to induce apoptosis and act as a tumour suppressor and inhibitor of TGF-β activity (Sandbothe et al., 2017). Furthermore, miR-449b down-regulates the translation of the transcription factor SOX-4, which facilitates TGF-β-induced EMT. Therefore, the up-regulation of miR-449b by sera from DN patients may be an adaptive response to an increased expression of TGF-β. Further experiments are required to measure TGF-β levels in media from cells exposed to human sera.

miR-122-5p

At 24h miR-122-5p was up-regulated by sera from patients with stage 3a, 4 and 5 of CKD, and at 48h by sera of stages 3a, 3b and 4. miR-122-5p is classified by the Qiagen's miRNA array manual as a miRNA related to signal transduction, transcriptional regulation and inflammation. It appears to be a liver specific miRNA related to fibrosis with unknown renal expression. The expression of miR-122-5p

seems to be negatively correlated with liver fibrosis by recruiting $CD11b^{hi}GR1^{+}$ inflammatory cells through targeting the Ccl2 chemokine (Bandiera et al., 2015). Similarly to miR-449b, it may be upregulated in the HK-2 cells as an adaptive response to injury.

miR-150-5p

miR-150-5p was up-regulated in both stages 3b and 5 after 24h exposure to human serum. Interestingly, after 48h incubation miR-150-5p was the only target down-regulated by sera of all stages of CKD (3a-5). miR-150-5p is described by the Qiagen's miRNA array manual as an angiogenesis miRNA. Overexpression of miR-150 significantly reduces the expression of the antifibrotic protein suppressor of cytokine signalling 1 (SOCS1) (H. Zhou et al., 2013). SOCS1 supresses the activity of TGF-β, which, as previously discussed, is key in ECM production. As well as suppressing TGF-β, SOCS1 also inhibits Interleukin-1β-induced Collagen I in the proximal tubule cells (H. Zhou et al., 2013).

miR-199b-5p

From the MIHS-117 PCR array the miRNA miR-199b is described as a pro-fibrotic, extracellular matrix remodelling and cell adhesion miRNA as well as being related to Epithelial-to-Mesenchymal Transition (EMT). It was up-regulated in stages 3a, 4 and 5 after 48 h of exposure to patient sera. Evidence demonstrates that when overexpressed, miR-199b plays a key role in liver and cardiac fibrosis by controling both Transforming Growth Induced factor (TGIF) and SMAD specific E3 ubiquitin protein ligase 2 (SMURF2e) (Duygu et al., 2017). These play pivotal roles in the TGF-β pathway which is a key regulator of ECM accumulation.

Interestingly, miR-199b is down-regulated after 24h of exposure to stage 3a patient sera.

miR-223-3p

miR-223-3p is related to signal transduction and transcriptional regulation, and is upregulated after exposure to sera from stage 3a, 3b and 5 patients. miR-223-3p regulates myeloid progenitor proliferation indicating that this miRNA may contribute to renal fibrosis by inducing macrophage activation (Zarjou et al., 2011). miR-223-3p is activated by CCAAT-enhancer-Binding Proteins binding to the miRNA promoter which in turn will promote granulocyte differentiation (Taibi et al., 2014).

miR-338-5p

miR-338-5p is a pro-fibrotic miRNA and was upregulated after 24 hours in cells exposed to sera from stage 3a and 3b patients. There has been little research into the activity of miR-338-5p in CKD but there is evidence that it promotes an inflammatory response by down-regulating SPRY1 leading to the increased expression of pro-inflammatory chemokines (Yang et al., 2017). There is also research showing that miR-338-5p may promote the expression of NF-κB1 which will lead to expression of pro-inflammatory molecules and chemokines (Ma et al., 2016).

miR-377-3p

The pro-fibrotic miR-377-3p was upregulated after 24 hours of exposure to stage 3a, 4 and 5 patient sera. This miRNA may be a suitable target in DN, as miR-337-3p has been found to be overexpressed in human mesangial cells when exposed to high levels of glucose (Q. Wang et al., 2008). The upregulation of miR-377-3p is related to an increased expression of fibronectin, which are a hallmark of DN (Q. Wang et al., 2008). It has been suggested that a target of this miRNA is PAK1 which can activate MAPK and NF-κB (Kato et al., 2009).

mir-491-5p

Sera from stage 3a, 3b and 4 upregulated the expression of miR-491-5p which is described as a miRNA related to signal transduction and transcriptional regulation. It has been found that upregulation of miR-491-5p is related to disruption of epithelial cell junctions and that high levels of TGF-β induce the expression of miR-491 through a MEK/p38 kinase pathway (Q. Zhou et al., 2010). The miR-491-5p then targets Par-3 expression which is essential in maintaining tight junctions within epithelial cells. This disruption is seen in DN and also contributes to EMT (Q. Zhou et al., 2010).

miR-874-3p

Epithelial-to-Mesenchymal transition is a function that miR-874-3p is related to according to appendix 2. It was upregulated in stages 3a and 5. The function of miR-874-3p in CKD is not fully documented but there is evidence that miR-874-3p inhibits EMT, as it targets SOX12 in hepatocellular carcinoma. SOX12 induces EMT by transactivating Twist1 and FGFBP1 expression which in turn inhibits E-Cadherin expression (T. Jiang et al., 2017). There is also evidence that miR-874-3p targets and inhibits CDK9 expression (L. Wang et al., 2014). CDK9 forms complexes with SMAD3 and SMAD4 to promote renal fibrosis by stimulating Collagen-1 promoter activity (Qu et al., 2015). The upregulation of miR-874-3p in HK-2 cells may be an adaptive response to the serum exposure.

4.5.2 Down-regulated miRNAs after 24 h and 48 h exposure to human sera

miR-217

According to the MIHS-117 Human Fibrosis miRNA PCR array from Sabiosciences, miR-217 is categorised as a miRNA related to extracellular matrix remodelling and cell adhesion. The results show that it is downregulated by at least 100 fold in stages 3a, 4 and also in stage 3b after 24 hours. Underexpression of miR-217 has been linked to various cancers such as gastric and ovarian cancer (Zheng et al., 2017) as it inhibits cell growth and metastasis and has a tumour suppressor role. This has also been observed in clear cell renal cell carcinoma (ccRCC) where downregulation of miRNA-217 was observed when compared to normal tissue (Li et al., 2013).

The expression of miR-217 is negatively correlated with SirT1 expression. SirT1 is involved in fibrosis by activating two major cell surface receptors: epidermal growth factor receptor (EGFR) and platelet-derived growth factor receptor-β (PDGFRβ), which are essential in renal fibroblast activation and proliferation (Ponnusamy et al., 2014). It has been shown in that study that inhibition of SirT1 blocked the phosphorylation of EGFR and PDGFRβ thus inhibiting fibroblast activity and proliferation.

miR-217 is also related to fibrosis in human renal proximal tubule cells. The downregulation of miR-217 is related to the downregulation of the dopamine D2 receptor (D_2R) which increases the susceptibility to renal inflammation (Han et al., 2015). The downregulated D_2R caused the downregulation of miR-217, which in turn increased the expression of TGF-β1, MMP-3 and Collagen-I all of which contribute to the progressive accumulation of ECM during TIF.

The significant downregulation of miR-217 in the CKD patients agrees with previous research in that the activities of miR-217 and the mechanisms that it is involved in contribute heavily to TIF.

miR-372-3p

Classified by the MIHS-117 PCR array as a miRNA related to signal transduction and transcriptional regulation, miR-372 is down-regulated in CKD stages 3a, 3b and 4 at 48h when compared to volunteers. Research has suggested that miR-372 can act as a tumour suppressor by inhibiting the function of the *ATAD2* gene which results in a G1 phase arrest and reduction of cell migration and invasion (Wu et al., 2014). ATAD2 is an oncogene that is frequently expressed in cancers and assists in cell proliferation and invasion through mechanisms involving genes such as *APC* and *CTNNA1*. The underexpression of miR-372 in the CKD patients must be allowing heightened expression of ATAD2 and contributing to the progressing fibrosis (Wu et al., 2014).

miR-215-5p

After 48 hours miR-215-5p was down-regulated by serum from patients with stage 3a CKD, miR-215-5p is related to both Pro-Fibrosis and Epithelial-to-Mesenchymal Transition. It is thought that down-regulation of miR-215-5p increases the proliferation in primary fibroblast cells by targeting two proteins that are related to cell cycling, Minichromosome Maintainance 10 (MCM10) and Cell Division Cycle 25A (CDC25A) (Lan et al., 2015). MCM10 promotes helicase activation by binding to single stranded DNA. As the helicase is involved in the G1/S phase of the cell cycle, reduction in helicase activity will restrict cell proliferation (Lan et al., 2015). CDC25A dephosphorylates Cylin-Dependent Kinase (CDK) 1 and 2 which in turn will progress the cell cycle. Overexpression of either of these proteins has been linked to various cancers so the expression of miR-215-5p is most likely intended to prevent excessive cell proliferation (Lan et al., 2015).

There is also research supporting that the down-regulation of miR-215-5p promotes EMT. One of the targets of miR-215-5p is Zinc finger E-box-binding homeobox 2 (ZEB2) which induces EMT by reducing E-cadherin activity (Hou et al., 2015). This so far has only been researched in lung cancers so further research is required to examine the effect in kidney disease.

4.6 miRNA expression in stage 5 samples

As discussed the viability results show a decreased viability in the stage 5 samples and this is reflected in the miRNA expression results. There are fewer miRNA up/down-regulations in stage 5 samples when compared to the volunteer samples especially with some of the fibrosis related miRNAs. For example miR-217 plays a key role in fibrosis and is severely downregulated in stages 3a, 3b and 4 but not in stage 5 where it is slightly upregulated. This could be that perhaps the stage 5 patients are undergoing dialysis due to decreased kidney function to filter out the pro-fibrotic factors, so the serum

samples may have been taken post-dialysis reducing the presence of these factors. However, as of the completion of this study, the dialysis status of these patients remained unknown.

4.7 Limitations of the project and future research

One of the limitations of this project relates to the preparation of patient and volunteer sera. The volunteers were recruited at MMU and their sera were isolated using BD Vacutainer® plastic serum tubes, whereas silica coated BD Vacutainer bottles with Hemogard stops were used for the isolation of patient sera. Although this could have led to some discrepancies in the results between volunteer and patient groups, the comparisons between patient groups have not been impacted.

Due to time and cost constraints, there were many elements of this project, which were not fully explored. During the miRNA fibrosis PCR arrays as well as exposing cells to the volunteers and CKD patients sera there were also cells exposed to SFM to be used as a control. However, due to logistic issues and time constraints it became unfeasible to analyse the SFM exposed cells in time.

When using the 50kDa and 100kDa ultrafiltration the results were inconclusive with the silver stains showing that there was not proper filtration. Significant amount of time was spent on the filtration experiments, as in the kidney the proximal tubular cells are only exposed to substances of 100 kDa or lower due to filtration in the glomerulus. According to the manufacturer's protocol of the 50 kDa the size of the filters was supposed to be at least 2x smaller than the target molecular weight cut off and purchasing further filters became unattainable due to time constraints.

When performing the assays using patient serum there was only 1 aliquot of serum per patient provided by the Salford Royal Trust. Due to this, there could be no repeats of any experiments. It would be beneficial for the research if the arrays could be repeated, and for perhaps extended to 72 hours to achieve a better understanding of the mechanisms over a longer time frame. A larger pool of healthy volunteers would also have increased the reliability of the control results.

During the arrays using CKD patient serum, conditioned cell media was harvested to be tested for cytokine expression. This would have added strength to the result, as certain cytokine expression is very important to the mechanisms of TIF. However, due to time constraints the assay was unable to be completed.

The next step for this research is to test the expression of key miRNAs in individual samples to confirm the results of the miRNA arrays which were obtained after pooling together volunteers or patients with the same CDK stage. Other areas to take the research further include looking into the impact of RAGE and AGEs on CKD, the expression of AGEs have an effect on DN and TIF so it would be interesting to analyse the levels expressed within the CKD stages.

5 Conclusions

Human serum influenced the expression of PAI-1 as can be seen in the gene reporter assay and Western blots. PAI-1 protein expression after 24 hours is increased as the CKD stages progress and it peaks with stage 4 serum exposures.

Sera from patients with DN produced different results from healthy volunteer sera, as demonstrated by the miRNA fibrosis assays. The various miRNAs that are under and overexpressed in the CKD patient serum in comparison to the volunteer serum are related to fibrosis and some of them may contribute to TIF (e.g. miR-217 and miR-449b). The relationship between TIF and miR-449b and other miRNA like miR-150 and miR-199b needs further research in this model of RPTEC exposed to sera from DN patients. This could be achieved by overexpressing and knocking out the miRNAs individually to measure the levels of markers of fibrosis like PAI-1 and TGF-β.

The data also consistently showed that the stage 5 CKD sera gave reduced levels of expression in PAI-1. It remains to be confirmed if the stage 5 patients underwent dialysis to filter out the CKD factors or the serum was isolated from pre-dialysis patients and contained cytotoxic/antiproliferative factors.

6 Appendix

6.1 Appendix 1: MIHS-117 miRNA PCR Array Human Fibrosis Layout from SabioSciences

hsa-let-7d-5p A01	hsa-miR-1-3p A02	hsa-miR-101-3p A03	hsa-miR-107 A04	hsa-miR-10a-5p A05	hsa-miR-10b-5p A06	hsa-miR-122-5p A07	hsa-miR-125b-5p A08	hsa-miR-126-3p A09	hsa-miR-129-5p A10	hsa-miR-132-3p A11	hsa-miR-133a-3p A12
hsa-miR-141-3p B01	hsa-miR-142-3p B02	hsa-miR-143-3p B03	hsa-miR-145-5p B04	hsa-miR-146a-5p B05	hsa-miR-146b-5p B06	hsa-miR-148a-3p B07	hsa-miR-150-5p B08	hsa-miR-155-5p B09	hsa-miR-15b-5p B10	hsa-miR-16-5p B11	hsa-miR-17-5p B12
hsa-miR-18a-5p C01	hsa-miR-192-5p C02	hsa-miR-194-5p C03	hsa-miR-195-5p C04	hsa-miR-196a-5p C05	hsa-miR-199a-5p C06	hsa-miR-199b-5p C07	hsa-miR-19a-3p C08	hsa-miR-19b-3p C09	hsa-miR-200a-3p C10	hsa-miR-200b-3p C11	hsa-miR-203a-3p C12
hsa-miR-204-5p D01	hsa-miR-208a-3p D02	hsa-miR-20a-5p D03	hsa-miR-211-5p D04	hsa-miR-215-5p D05	hsa-miR-21-5p D06	hsa-miR-216a-5p D07	hsa-miR-217 D08	hsa-miR-223-3p D09	hsa-miR-23a-3p D10	hsa-miR-25-3p D11	hsa-miR-26a-5p D12
hsa-miR-26b-5p E01	hsa-miR-27a-3p E02	hsa-miR-27b-3p E03	hsa-miR-29a-3p E04	hsa-miR-29b-3p E05	hsa-miR-29c-3p E06	hsa-miR-302b-3p E07	hsa-miR-30a-5p E08	hsa-miR-31-5p E09	hsa-miR-324-3p E10	hsa-miR-324-5p E11	hsa-miR-325 E12
hsa-miR-32-5p F01	hsa-miR-328-3p F02	hsa-miR-335-5p F03	hsa-miR-338-5p F04	hsa-miR-34a-5p F05	hsa-miR-372-3p F06	hsa-miR-375 F07	hsa-miR-377-3p F08	hsa-miR-378a-3p F09	hsa-miR-382-5p F10	hsa-miR-449a F11	hsa-miR-449b-5p F12
hsa-miR-451a G01	hsa-miR-491-5p G02	hsa-miR-5011-5p G03	hsa-miR-503-5p G04	hsa-miR-5692a G05	hsa-miR-590-5p G06	hsa-miR-661 G07	hsa-miR-663a G08	hsa-miR-744-5p G09	hsa-miR-7-5p G10	hsa-miR-874-3p G11	hsa-miR-92a-3p G12
cel-miR-39-3p H01	cel-miR-39-3p H02	SNORD61 H03	SNORD68 H04	SNORD72 H05	SNORD95 H06	SNORD96A H07	RNU6-6P H08	miRTC H09	miRTC H10	PPC H11	PPC H12

6.2 Appendix 2: Functional miRNA grouping in MIHS-117 PCR Fibrosis assay from SabioSciences

Pro-Fibrotic: miR-142-3p , miR-145-5p, miR-155-5p, miR-199b-5p, miR-21-5p, miR-215, miR-216a-5p, miR-27a-3p, miR-27b-3p, miR-32-5p, miR-338-5p, miR-34a-5p, miR-377-3p, miR-382-5p, miR-192-5p, miR-30a-5p, miR-208a, miR-5692a, miR-5011-5p.

Anti-Fibrotic: let-7d-5p, miR-107, miR-132-3p, miR-133a, miR-141-3p, miR-15b-5p, miR-16-5p, miR-17-5p, miR-18a-5p, miR-194-5p, miR-19a-3p, miR-19b-3p, miR-200a-3p, miR-200b-3p, miR-204-5p, miR-20a-5p, miR-211-5p, miR-26a-5p, miR-26b-5p, miR-29b-3p, miR-335-5p, miR-449a, miR-449b-5p, miR-590-5p, miR-92a-3p.

Extracellular Matrix Remodeling & Cell Adhesion: miR-199a-5p, miR-199b-5p, miR-29a-3p, miR-29b-3p, miR-29c-3p, miR-449a, miR-21-5p, miR-204-5p, miR-25-3p, miR-7-5p, miR-196a-5p, miR-203a, miR-27b-3p, miR-27a-3p, miR-451a, miR-145-5p, miR-143-3p, miR-1, miR-10a-5p, miR-10b-5p, miR-661, miR-30a-5p, miR-16-5p, miR-217.

Inflammation: let-7d-5p, miR-204-5p, miR-122-5p, miR-146a-5p, miR-199a-5p, miR-155-5p, miR-21-5p, miR-129-5p, miR-142-3p, miR-503-5p.

Angiogenesis: let-7d-5p, miR-378a-3p, miR-372, miR-34a-5p, miR-29b-3p, miR-20a-5p, miR-200b-3p, miR-195-5p, miR-17-5p, miR-16-5p, miR-15b-5p, miR-150-5p, miR-145-5p, miR-126-3p, miR-107, miR-31-5p, miR-375.

Signal Transduction & Transcriptional Regulation: miR-26a-5p, miR-18a-5p, miR-122-5p, miR-133a, miR-20a-5p, miR-203a, miR-19a-3p, miR-17-5p, miR-146a-5p, miR-155-5p, miR-92a-3p, miR-29b-3p, miR-141-3p, miR-29a-3p, miR-204-5p, miR-590-5p, miR-372, miR-302b-3p, miR-19b-3p, miR-21-5p, miR-1, miR-217, miR-23a-3p, miR-328, miR-744-5p, miR-148a-3p, miR-451a, miR-125b-5p, miR-449a, miR-34a-5p, miR-29c-3p, miR-195-5p, miR-192-5p, miR-16-5p, miR-15b-5p, miR-663a, miR-30a-5p, miR-378a-3p, miR-145-5p, miR-146b-5p, miR-27a-3p, miR-324-5p, miR-324-3p, miR-223-3p, miR-491, miR-101-3p, miR-491-5p.

Epithelial-to-Mesenchymal Transition: let-7d-5p, miR-107, miR-155-5p, miR-199a-5p, miR-199b-5p, miR-200a-3p, miR-200b-3p, miR-215, miR-29a-3p, miR-29b-3p, miR-29c-3p, miR-382-5p, miR-325, miR-874.

7 References:

August, P. and Suthanthiran, M. (2003) 'Transforming growth factor beta and progression of renal disease: Management of comorbidities in kidney disease in the 21st century: Anemia and bone disease.' *Kidney International*, 64(Supplement 87) pp. S99-S104.

Bandiera, S., Pfeffer, S., Baumert, T. F. and Zeisel, M. B. (2015) 'miR-122 - A key factor and therapeutic target in liver disease.' *Journal of Hepatology*, 62(2) pp. 448-457.

Baumann, V. and Winkler, J. (2014) 'miRNA-based therapies: Strategies and delivery platforms for oligonucleotide and non-oligonucleotide agents.' *Future Medicinal Chemistry*, 6(17) 4 May 2015, pp. 1967-1984.

Bergstrom, M., Falk, P. and Holmdahl, L. (2006) 'Effect of Acidosis on Expression of Mesothelial Cell Plasminogen Activator Inhibitor Type-1.' *Surgical Endoscopy*, 20(9) 26 May 2006, pp. 1448-1452.

Brohem, C. A., de Carvalho, C. M., Radoski, C. L., Santi, F. C., Baptista, M. C., Swinka, B. B., de A Urban, C., de Araujo, L. R., Graf, R. M., Feferman, I. H. and Lorencini, M. (2013) 'Comparison between fibroblasts and mesenchymal stem cells derived from dermal and adipose tissue.' *International Journal of Cosmetic Science*, 35(5) 27 June 2013, pp. 448-457.

Caramori, M. L., Fioretto, P. and Mauer, M. (2003) 'Low Glomerular Filtration Rate in Normoalbuminuric Type 1 Diabetic Patients.' *Diabetes*, 52(4) p. 1036.

Chen, C. and Raghunath, M. (2009) 'Focus on collagen:*in vitro* systems to study fibrogenesis and antifibrosis _ state of the art.' *Fibrogenesis and Tissue Repair*, 2(7) 15 December 2009,

Dervisoglu, E., Kozdag, G., Etiler, N. and Kalender, B. (2012) 'Association of glomerular filtration rate and inflammation with left ventricular hypertrophy in chronic kidney disease patients.' *Hippokratia*, 16(2) pp. 137-142.

Duran-Salgado, M. B. and Rubio-Guerra, A. F. (2014) 'Diabetic nephropathy and inflammation.' *World Journal of Diabetes*, 5(3) 15 June 2014, pp. 393-398.

Duygu, B., Poels, E. M., Juni, R., Bitsch, N., Ottaviani, L., Olieslagers, S., de Windt, L. J. and da Costa Martins, P. A. (2017) 'miR-199b-5p is a regulator of left ventricular remodeling following myocardial infarction.' *Non-coding RNA Research*, 2(1) pp. 18-26.

Eddy, A. A. and Fogo, A. B. (2006) 'Plasminogen Activaor Inhibitor-1 in Chronic Kidney Disease: Evidence and Mechanisms of Action.' *Journal of the American Society of Nephrology*, 17(11) October 11, 2006, pp. 2999-3012.

Efstratiadis, G., Divani M, K. E. and Vergoulas, G. (2009) 'Renal Fibrosis.' *Hippokratia*, 13(4) pp. 224-229.

Farris, A. and Colvin, R. (2012) 'Renal Interstitial Fibrosis: Mechanisms and Evaluation In: Current Opinion in Nephrology and Hypertension.' *Current Opinion in Nephrology and Hypertension*, 21(3) 1st May 2013, pp. 289-300.

Fujigaki, Y., Muranaka, Y., Sun, D., Goto, T., Zhou, H., Sakakima, M., Fukasawa, H., Yonemura, K., Yamamoto, T. and Hishida, A. (2005) 'Transient myofibroblast differentiation of interstitial fibroblastic cells relevant to tubular dilatation in uranyl acetate-induced acute renal failure in rats.' *Virchows Archiv*, 446(2) 18 December 2004, pp. 164-176.

Gansevoort, R. T., Correa-Rotter, R., Hemmelgarn, B. R., Jafar, T. H., Heerspink, H. J. L., Mann, J. F., Matsushita, K. and Wen, C. P. (2013) 'Chronic kidney disease and cardiovascular risk: epidemiology, mechanisms, and prevention.' *The Lancet*, 382(9889) 27 July 2013, pp. 339-352.

Gentle, M. E., Shi, S., Daehn, I., Zhang, T., Qi, H., Yu, L., D'Agati, V. D., Schlondorff, D. O. and Bottinger, E. P. (2013) 'Epithelial Cell TGF*β* Signaling Induces Acute Tubular Injury and Interstitial Inflammation.' *Journal of the American Society of Nephrology*, 24(5) 28 March 2013, pp. 787-799.

Ghosh, A. K. and Vaughan, D. E. (2012) 'PAI-1 in Tissue Fibrosis.' *Journal of Cellular Physiology*, 227(2) February 1 2013, pp. 493-507.

Ha, M. and Kim, V. N. (2014) 'Regulation of microRNA biogenesis.' *Nat Rev Mol Cell Biol*, 15(8), 08//print, pp. 509-524.

Han, F., Konkalmatt, P., Chen, J., Gildea, J., Felder, R. A., Jose, P. A. and Armando, I. (2015) 'miR-217 Mediates the Protective Effects of the Dopamine D2 Receptor on Fibrosis in Human Renal Proximal Tubule Cells.' *Hypertension*, 2015(65) 23 March 2015, pp. 1118-1125.

Hou, Y., Zhen, J., Xu, X., Zhen, K., Zhu, B., Pan, R. and Zhao, C. (2015) 'miR-215 functions as a tumor suppressor and directly targets ZEB2 in human non-small cell lung cancer.' *Oncology Letters*, 10(4) 11 August 2015, pp. 1985-1992.

Hruska, K. A., Matthew, S., Lund, R., Qiu, P. and Pratt, R. (2008) 'Hyperphosphatemia of Chronic Kidney Disease.' *Kidney International*, 74(2) 31 August 2009, pp. 148-157.

Huang, S. T., Shu, K. H., Cheng, C. H., Wu, M. J., Yu, T. M., Chuang, Y. W. and Chen, C. H. (2012) 'Serum total p-cresol and indoxyl sulfate correlated with stage of chronic kidney disease in renal transplant recipients.' *Transplantation proceedings*, 44(3) pp. 621-624.

Jefferson, J. A., Shankland, S. J. and Pichler, R. H. 'Proteinuria in diabetic kidney disease: A mechanistic viewpoint.' *Kidney International*, 74(1) pp. 22-36.

Jiang, T., Guan, L. Y., Ye, Y. S., Liu, H. Y. and Li, R. (2017) 'MiR-874 inhibits metastasis and epithelial-mesenchymal transition in hepatocellular carcinoma by targeting *SOX12*.' *American Journal of Cancer Research*, 7(6) 1 June 2017, pp. 1310-1321.

Jiang, X., Tsitsiou, E., Herrick, S. E. and Lindsay, M. A. (2010) 'microRNAs and the regulation of fibrosis.' *The FEBS journal*, 277(9) 1 May 2011, pp. 2015-2021.

Kasti, S. P., Speidl, W. S., Kaun, C., Rega, G., Assadian, A., Weiss, T. W., Valent, P., Hagmueller, G. W., Maurer, G., Huber, K. and Wojta, J. (2006) 'The complement component C5a induces the expression of plasminogen activator inhibitor-1 in human macrophages via NF-kappaB activation.' *Journal of Thrombosis and Haemostasis*, 4(8) 4 August 2006, pp. 1790-1797.

Kato, M., Arce, L. and Natarajan, R. (2009) 'MicroRNAs and Their Role in Progressive Kidney Diseases.' *Clinical Journal of the American Society of Nephrology*, 4(7) pp. 1255-1266.

Kawarada, Y., Inoue, Y., Kawasaki, F., Fukuura, K., Sato, K., Tanaka, T., Itoh, Y. and Hayashi, H. (2016) 'TGF-β induces p53/Smads complex formation in the PAI-1 promoter to activate transcription.' 6, 10/19/online, p. 35483.

Kito, N., Endo, K., Ikesue, M., Weng, H. and Iwai, N. (2015) 'miRNA Profiles of Tubular Cells: Diagnosis of Kidney Injury.' *BioMed Research International*, 2015, 04/30, p. 465479.

Kurts, C., Panzer, U., Anders, H.-J. and Rees, A. J. (2013) 'The immune system and kidney disease: basic concepts and clinical implications.' *Nat Rev Immunol*, 13(10), 10//print, pp. 738-753.

Lan, W., Chen, S. and Tong, L. (2015) 'MicroRNA-215 Regulates Fibroblast Function: Insights from a Human Fibrotic Disease.' *Cell Cycle*, 14(12) 7 January 2015, pp. 1973-1984.

Lee, H. B. and Ha, H. (2005) 'Plasminogen activator inhibitor-1 and diabetic nephropathy.' *Nephrology*, 10(s2) 12 September 2005, pp. S11-S13.

Levey, A. S., Becker, C. and Inker, L. A. (2015) 'Glomerular Filtration Rate and Albuminuria for Detection and Staging of Acute and Chronic Kidney Disease in Adults: A Systematic Review.' *JAMA*, 313(8) 13th February 2015, pp. 837-846.

Li, H., Zhao, J., Zhang, J., Huang, Q., Huang, J., Chi, L., Tang, H., Liu, G., Zhu, D. and Ma, W. (2013) 'MicroRNA-217, down-regulated in clear cell renal cell carcinoma and associated with lower survival, suppresses cell proliferation and migration.' *Neoplasma*, 60(5) pp. 511-515.

Lim, A. K. (2014) 'Diabetic nephropathy – complications and treatment.' *International Journal of Nephrology and Renovascular Disease*, 2014(7) 15 October 2014, pp. 361-381.

Lin, H. H., Huang, C. C., Lin, T. Y. and Lin, C. Y. (2015) 'p-Cresol mediates autophagic cell death in renal proximal tubular cells.' *Toxicology Letters*, 234(1) 7 February 2015, pp. 20-29.

Loeffler, I. and Wolf, G. (2014) 'Transforming growth factor-β and the progression of renal disease.' *Nephrology Dialysis Transplantation*, 29(1) 1 February 2014, pp. 37-45.

Ma, X., He, X., Dong, P., Xue, D., Song, D., Xu, H. and Zhang, X. (2016) 'miR-338-5p modulates B cell biological functions by targeting NF-κB1.' *Chinese Journal of Cellular and Molecular Immunology*, 32(11) pp. 1475-1480.

Mason, R. M. and Wahab, N. A. (2003) 'Extracellular Matrix Metabolism in Diabetic Nephropathy.' *Journal of the American Society of Nephrology*, 14(5) pp. 1358-1373.

Medici, D. and Kalluri, R. (2012) 'Endothelial-mesenchymal transition and its contribution to the emergence of stem cell phenotype.' *Seminars in cancer biology*, 22(5-6) 1 October 2013, pp. 379-384.

Meran, S. and Steadman, R. (2011) 'Fibroblasts and myofibroblasts in renal fibrosis.' *International Journal of Experimental Pathology*, 92(3) June 2011, pp. 158-167.

Nasri, H. and Rafieian-Kopaei, M. (2015) 'Diabetes mellitus and renal failure: Prevention and management.' *Journal of Research in Medical Sciences*, 20(11) pp. 1112-1120.

Orang, A. V., Safaralizadeh, R. and Kazemzadeh-Bavili, K. (2014) 'Mechanisms of miRNA-Mediated Gene Regulation from Common Downregulation to mRNA-Specific Upregulation.' *International Journal of Genomics*, vol. 2014(Article ID 970607) 10 August 2014, p. 15 pages.

Patel, V. and Noureddine, L. (2012) 'MicroRNAs and Fibrosis.' *Current Opinion in Nephrology and Hypertension*, 21(4) 1 July 2012, p. 410.

Ponnusamy, M., Zhou, X., Yan, Y., Tang, J., Tolbert, E., Zhao, T., Gong, R. and Zhuang, S. (2014) 'Blocking Sirtuin 1 and 2 Inhibits Renal

Interstitial Fibroblast Activation and Attenuates Renal Interstitial

Fibrosis in Obstructive Nephropathy.' *The Journal of Pharmacology and Experimental Thereapeutics*, 350(2) pp. 243-256.

Qu, X., Jiang, M., Sun, Y. B., Jiang, X., Fu, P., Ren, Y., Wang, D., Dai, L., Caruana, G., Bertram, J. F., Nikolic-Paterson, D. J. and Li, J. (2015) 'The Smad3/Smad4/CDK9 complex promotes renal fibrosis in mice with unilateral ureteral obstruction.' *Kidney International*, 88(6) 29 July 2015, pp. 1323-1335.

Ruggiero, A., Villa, C. H., Bander, E., Rey, D. A., Bergkvist, M., Batt, C. A., Manova-Todorova, K., Deen, W. M., Scheinberg, D. A. and McDevitt, M. R. (2010) 'Paradoxical glomerular filtration of carbon nanotubes.' *Proceedings of the National Academy of Sciences of the United States of America*, 107(27) 21 June 2010, pp. 12369-12374.

Sakai, N., Furuichi, K., Shinozaki, Y., Yamauchi, H., Toyama, T., Kitajima, S., Okumura, T., Kokubo, S., Kobayashi, M., Takasawa, K., Takeda, S.-i., Yoshimura, M., Kaneko, S. and Wada, T. (2010) 'Fibrocytes are involved in the pathogenesis of human chronic kidney disease.' *Human Pathology*, 41(5), 2010/05/01/, pp. 672-678.

Sandbothe, M., Buurman, R., Reich, N., Greiwe, L., Vajen, B., Gurlevik, E., Schaffer, V., Eilers, M., Kuhnel, F., Vaquero, A., Longerich, T., Roessler, S., Schirmacher, P., Manns, M., Illig, T., Schlegelberger, B. and Skawran, B. (2017) 'The microRNA-449 family inhibits TGF-β-mediated liver cancer cell migration by targeting SOX4.' *Journal of Hepatology*, 66(5) 11 January 2017, pp. 1012-1021.

Schnaper, H. W. (2014) 'Remnant nephron physiology and the progression of chronic kidney disease.' *Pediatric nephrology (Berlin, Germany)*, 29(2), 05/29, pp. 10.1007/s00467-00013-02494-00468.

Shi, M. A. and Shi, G. P. (2011) 'Intracellular Delivery Strategies for MicroRNAs and Potential Therapies for Human Cardiovascular Diseases.' *Science Signalling*, 3(146) 29 March 2011,

Suzuki, M., Akimoto, K. and Hattori, Y. (2002) 'Glucose upregulates plasminogen activator inhibitor-1 gene expression in vascular smooth muscle cells.' *Life Sciences*, 72(1) pp. 59-66.

Taibi, F., Metzingeer-Le Meuth, V., Massey, Z. A. and Metzinger, L. (2014) 'miR-223: An inflammatory oncomiR enters the cardiovascular field.' *Biochimica et Biophysica Acta (BBA) - Molecular Basis of Disease*, 1842(7) 18 March 2014, pp. 1001-1009.

Tang, S. C. W. and Neng Lai, K. (2012) 'The pathogenic role of the renal proximal tubular cell in diabetic nephropathy.' *Nephrology Dialysis Transplantation*, 27(8) 1st August 2012, pp. 3049-3056.

Thomas, R., Kanso, A. and Sedor, J. R. (2008) 'Chronic Kidney Disease and Its Complications.' *Primary Care*, 35(2) 1st June 2009, pp. 329-vii.

Tojo, A. and Kinugasa, S. (2012) 'Mechanisms of Glomerular Albumin Filtration and Tubular Reabsorption.' *International Journal of Nephrology*, vol. 2012(Article ID 481520) 21 March 2012, p. 9 pages.

Van der Hauwaert, C., Savary, G., Gnemmi, V., Glowacki, F., Pottier, N., Bouillez, A., Maboudou, P., Zini, L., Leroy, X., Cauffiez, C., Perrais, M. and Aubert, S. (2013) 'Isolation and Characterization of a Primary Proximal Tubular Epithelial Cell Model from Human Kidney by CD10/CD13 Double Labeling.' *PLoS ONE*, 8(6) 14th June 2013,

Wahid, F., Shehzad, A., Khan, T. and Kim, Y. (2010) 'MicroRNAs: Synthesis, mechanism, function, and recent clinical trials.' *Biochimica et Biophysica Acta (BBA) - Molecular Cell Research*, 1803(11) 13 June 2010, pp. 1231-1243.

Wang, L., Gao, W., Hu, F., Xu, Z. and Wang, F. (2014) 'MicroRNA-874 inhibits cell proliferation and induces apoptosis in human breast cancer by targeting CDK9.' *FEBS Letters*, 588(24) 20 December 2014, pp. 4527-4535.

Wang, Q., Wang, Y., Minto, A. W., Wang, J., Shi, Q., Li, X. and Quigg, R. J. (2008) 'MicroRNA-377 is up-regulated and can lead to increased fibronectin production in diabetic nephropathy.' *The FASEB Journal*, 22(12) pp. 4126-4135.

Wolf, G. (2006) 'Renal injury due to renin–angiotensin–aldosterone system activation of the transforming growth factor-β pathway.' *Kidney International*, 70(11), 2006/12/01/, pp. 1914-1919.

Wu, G., Liu, H., He, H., Wang, Y., Lu, X., Yu, Y., Xia, S., Meng, X. and Liu, Y. (2014) 'miR-372 down-regulates the oncogene ATAD2 to influence hepatocellular carcinoma proliferation and metastasis.' *BMC Cancer*, 14(107) 19 February 2014,

Yan, J., Zhang, Z., Jia, L. and Wang, Y. (2016) 'Role of Bone Marrow-Derived Fibroblasts in Renal Fibrosis.' *Frontiers in Physiology*, 7(61) 25 February 2016,

Yang, Y., Wang, Y., Liang, Q., Yao, L., Gu, S. and Bai, X. (2017) 'MiR-338-5p Promotes Inflammatory Response of Fibroblast-Like Synoviocytes in Rheumatoid Arthritis via Targeting SPRY1.' *Journal of Cellular Biochemistry*, 118(8) 3 March 2017, pp. 2295-2301.

Yildiz, S. Y., Kuru, P., Oner, E. T. and Agirbasli, M. (2014) 'Functional Stability of Plasminogen Activator Inhibitor-1.' *The Scientific World Journal*, Vol. 2014(Article ID 858293) 15 October 2014, p. 11 pages.

Zarjou, A., Yang, S., Abraham, E., Agarwal, A. and Liu, G. (2011) 'Identification of a microRNA signature in renal fibrosis: role of miR-21.' *American Journal of Physiology-Renal Physiology*, 301(4) 20 July 2011, pp. F793-F801.

Zeisberg, M. and Neilson, E. G. (2009) 'Biomarkers for epithelial-mesenchymal transitions.' *The Journal of Clinical Investigation*, 119(6), 06/01, pp. 1429-1437.

Zeisberg, M. and Neilson, E. (2010) 'Mechanisms of Tubulointerstitial Fibrosis.' *Journal of the American Society of Nephrology*, 21(11) September 23, 2010, pp. 1819-1834.

Zeisberg, M. and Kalluri, R. (2015) 'Physiology of the Renal Interstitium.' *Clinical Journal of the American Society of Nephrology*, 10(10) 26 March 2015, pp. 1831-1840.

Zhang, J. and An, J. (2007) 'Cytokines, Inflammation and Pain.' *International anesthesiology clinics*, 45(2) 30 november 2009, pp. 27-37.

Zhao, H., Dong, Y., Tian, X., Tan, T. K., Liu, Z., Zhao, Y., Zhang, Y., Harris, D. C. H. and Zheng, G. (2013) 'Matrix metalloproteinases contribute to kidney fibrosis in chronic kidney diseases.' *World Journal of Nephrology*, 2(3) 6 August 2013, pp. 84-89.

Zheng, J., Liu, X., Xue, Y., Gong, W., Ma, J., Xi, Z., Que, Z. and Liu, Y. (2017) 'TTBK2 circular RNA promotes glioma malignancy by regulating miR-217/HNF1β/Derlin-1 pathway.' *Journal of Hematology & Oncology*, 10(52) 20 February 2017,

Zhou, H., Hasni, S. A., Perez, P., Tandon, M., Jang, S., Zheng, C., Kopp, J. B., Austin III, H., Balow, J. E., Alevizos, I. and Illei, G. G. (2013) 'miR-150 Promotes Renal Fibrosis in Lupus Nephritis by

Downregulating SOCS1.' *Journal of the American Society of Nephrology*, 24(7) 28 June 2013, pp. 1073-1087.

Zhou, Q., Fan, J., Ding, X., Peng, W., Yu, X., Chen, Y. and Nie, J. (2010) 'TGF-β-induced MiR-491-5p Expression Promotes Par-3 Degradation in Rat Proximal Tubular Epithelial Cells.' *The Journal of Biological Chemistry*, 285 21 October 2010, pp. 40019-40027.